Marine and Petroleum Geology 98 (2018) 815–835

Contents lists available at ScienceDirect

Marine and Petroleum Geology

journal homepage: www.elsevier.com/locate/marpetgeo

Research paper

Pore pressure and reservoir quality evolution in the deep Taranaki Basin, New Zealand

Sean R. O'Neill[a,*], Stuart J. Jones[a,**], Peter J.J. Kamp[b], Richard E. Swarbrick[a,c], Jon G. Gluyas[a]

[a] Department of Earth Sciences, Durham University, DH1 3LE, UK
[b] School of Science, University of Waikato, Hamilton, New Zealand
[c] Swarbrick GeoPressure Consultancy Ltd, Durham, UK

ARTICLE INFO

Keywords:
Overpressure
Diagenesis
Basin modelling
Reservoir quality
Lateral drainage
Pore pressure
Tectonostratigraphy

ABSTRACT

The Palaeocene fluvial to shallow marine sandstones of the Farewell Formation are an important proven hydrocarbon reservoir in the Taranaki Basin, New Zealand. The Kapuni Deep-1 well was drilled to target Farewell Formation sandstones in the deeper overpressured (> 5000 m, > 3000 psi/21 MPa) sections of the onshore Manaia Graben of the Taranaki Basin. However, the Farewell Formation sandstones display anomalously low measured helium porosities (1–4.5%) and intergranular volumes (6–11%) even for their present-day, close to maximum, burial depth (c.5000 m). One dimensional burial history modelling demonstrates initial rapid burial leading to significant porosity reduction via mechanical compaction, enhanced by poor sorting, angular grain morphology and the presence of ductile grains, which allowed efficient packing and plastic deformation. Low intergranular volume (IGV), anhedral nature of quartz overgrowths, a general lack of fluid inclusions, and poor crystalline clay mineral content indicate that early burial compactional processes significantly influenced reservoir quality.

The lack of mudstone to siltstone grade lithologies within the overlying Eocene section inhibited the early or shallow onset of overpressure in the Farewell Formation. One dimensional basin modelling has shown that rapid Pliocene subsidence related to exceptionally high sedimentation rates generated overpressure through disequilibrium compaction in the overlying Oligocene to early Miocene section during the past 6 Ma. However, the late and deep (> 3000 m) onset of overpressure had no effect on arresting porosity loss in the Farewell Formation. Continued compaction of Farewell Formation sandstones after dissolution of early carbonate cements of CO_2 rich fluids creates zones of extremely low permeability, which have the potential to act with interbedded shales to form pressure seals as seen in the Kapuni Field.

1. Introduction

Eocene clastic reservoirs within the Manaia Graben of Taranaki Basin, New Zealand (Fig. 1), display enhanced reservoir quality through local preservation of secondary porosity, generated by feldspar dissolution due to migration of large volumes of CO_2 rich fluids through permeable beds (Higgs et al., 2013). The Kapuni gas condensate field (Fig. 1) in the Manaia Graben produces natural gas (methane) and CO_2 from two Eocene reservoirs. In 1983 an exploration well, Kapuni Deep-1, was drilled in an attempt to increase the field's reserves by testing the reservoir potential of the deeply buried and overpressured (> 5000 m, > 3000 psi/21 MPa) Palaeocene Farewell Formation (Fig. 2). As the CO_2 content is partly sourced from underlying Cretaceous strata (Figs. 2 and 3), it could be expected that the Farewell Formation would display similar enhanced reservoir quality due to the updip migration of CO_2 towards the crest of the Kapuni structure.

Kapuni Deep-1 encountered sandstone beds in the Farewell Formation (Fig. 2) with extremely poor reservoir quality, exhibiting a measured porosity of between 1 and 4.5% and a permeability of 0.1–0.25 mD. Measured helium core plug porosity data for Farewell Formation reservoirs from across the Taranaki Basin (Higgs et al., 2012) and the associated compaction curves for varying ductile grain contents (Worden et al., 1997) are shown in Fig. 4. Since the Farewell Formation at Kapuni Deep-1 is comprised of 5% ductile grains, measured porosity data are significantly off trend, and display anomalously low porosity for its current burial depth. The compaction curves do not account for the impact of diagenetic cements or effective stress history; these aspects and others will be discussed when investigating mechanisms for the exceptionally low reservoir quality of the sandstone beds in the Farewell Formation.

* Corresponding author.
** Corresponding author.
E-mail addresses: sean.oneill@durham.ac.uk (S.R. O'Neill), stuart.jones@durham.ac.uk (S.J. Jones).

https://doi.org/10.1016/j.marpetgeo.2018.08.038
Received 22 April 2018; Received in revised form 29 August 2018; Accepted 30 August 2018
Available online 31 August 2018

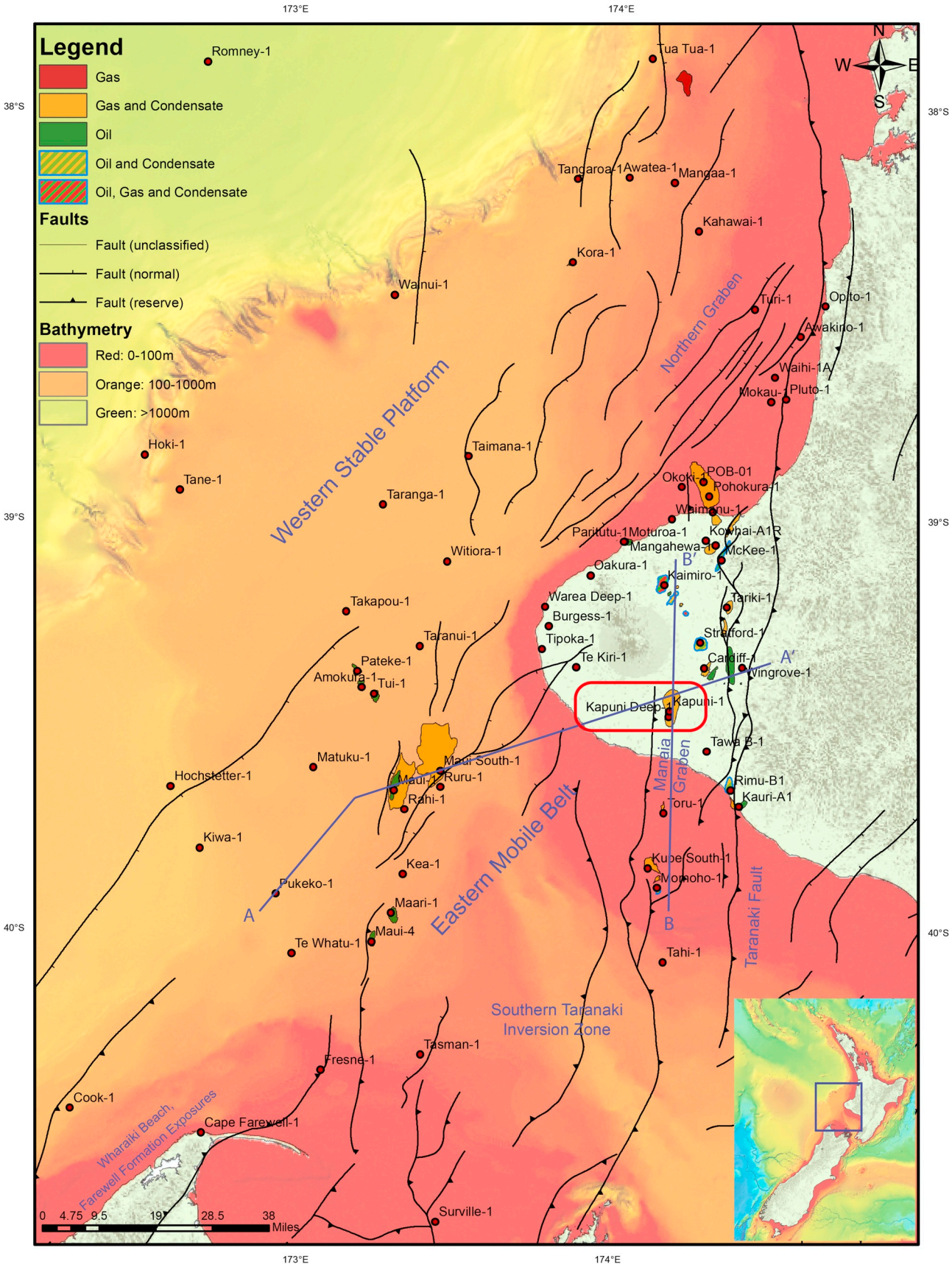

Fig. 1. Map of Taranaki Basin displaying key wells, producing fields, structure and bathymetry. For location of line A-A′ see Fig. 3 and line B-B′ see Fig. 14. Red Box – location of Kapuni Field and Kapuni Deep-1 (bathymetry after Mitchell et al., 2012). (For interpretation of the references to colour in this figure legend, the reader is referred to the Web version of this article.)

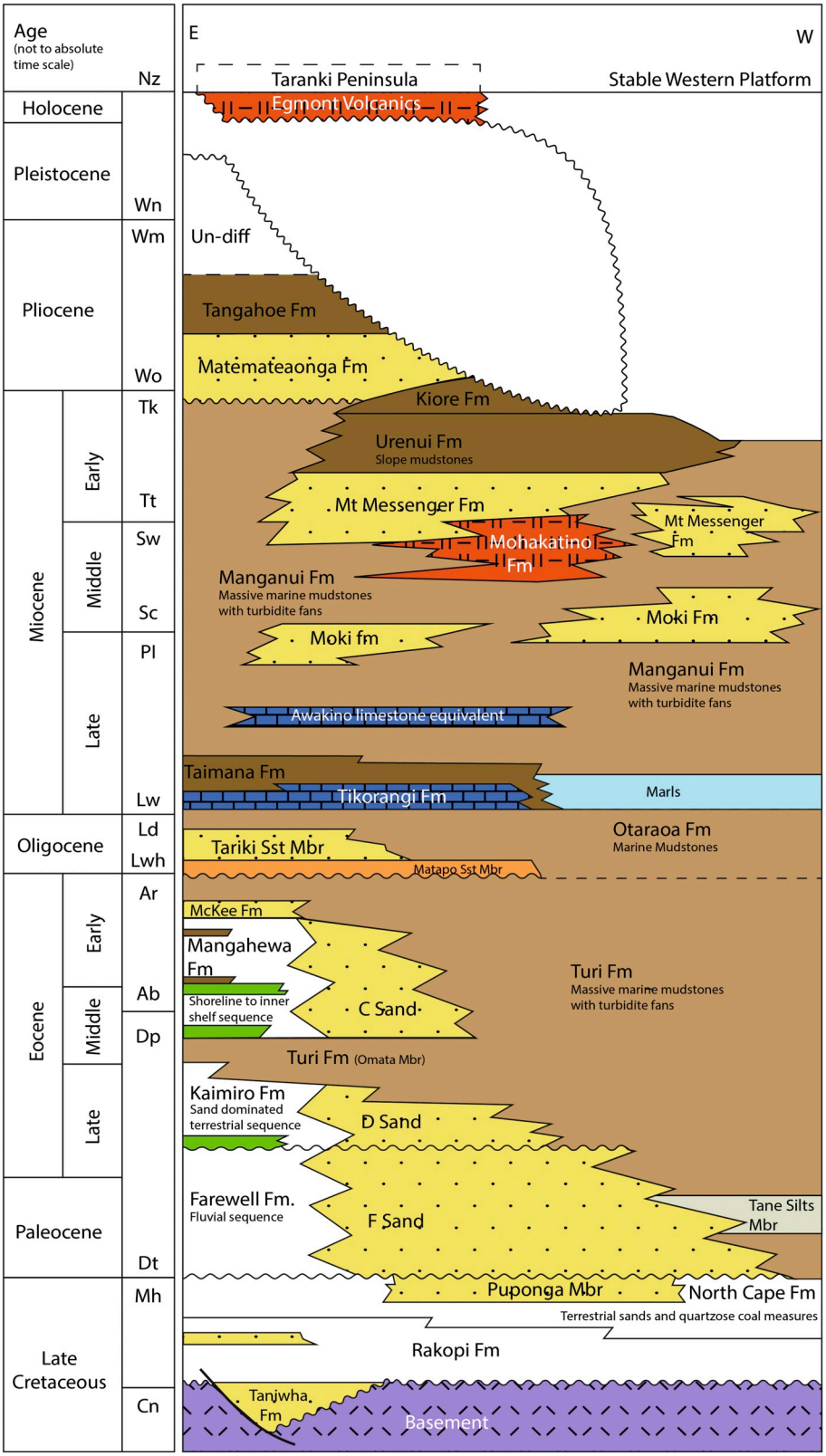

Fig. 2. Subsurface stratigraphy of Taranaki Peninsula through Kapuni Field, Taranaki Basin (modified from (King and Thrasher, 1996).

Hydrocarbon producing basins that display shallow onset and the maintenance of high pore fluid pressure (i.e. low vertical effective stress (VES)) have been shown to preserve anomalously high porosity (> 30%) at significant depth (> 5000 m) by lessening the impact of mechanical compaction (Grant et al., 2014; Nguyen et al., 2013; Sathar and Jones, 2016; Stricker et al., 2016). In this study a one dimensional basin model has been constructed to investigate the onset and subsequent development of overpressure, and the increase of temperature through burial. Pressure data reported for Kapuni Deep-1 are used to investigate vertical pressure distribution in the section encountered by

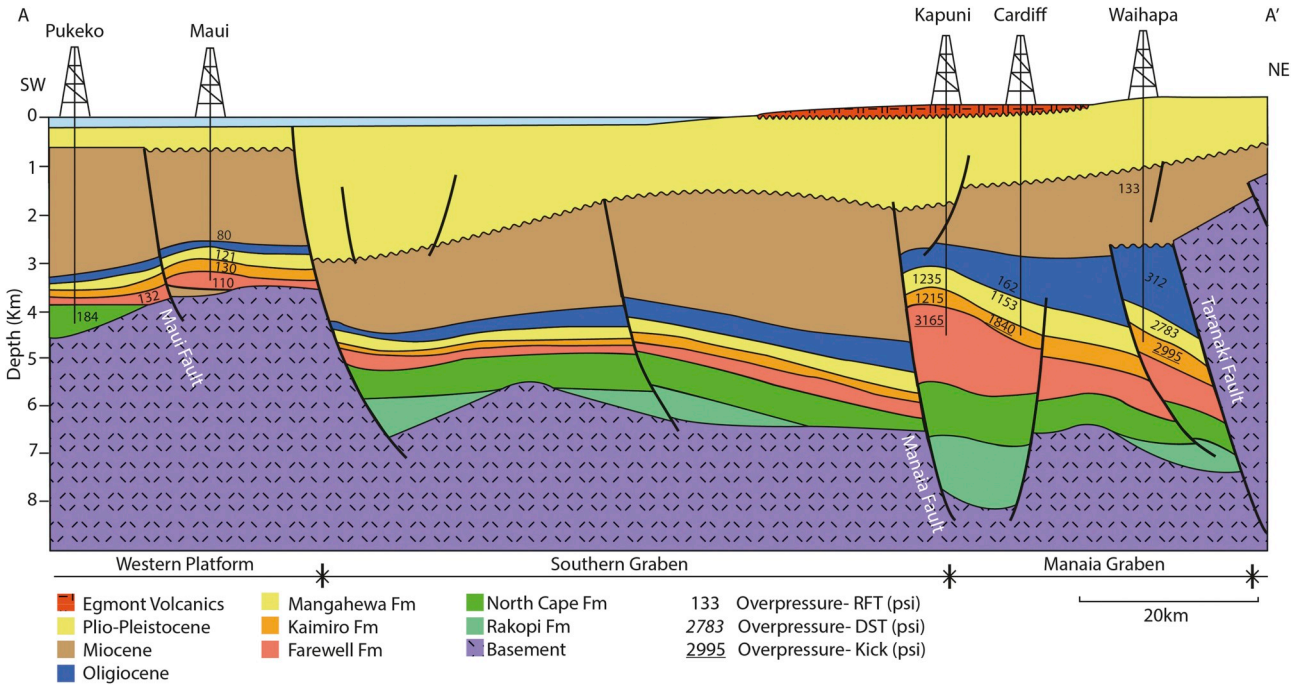

Fig. 3. Cross section (line A-A′, Fig. 1) displays lateral and vertical pressure variations (Modified from (King and Thrasher, 1996).

the well and to calibrate the basin modelling parameters. A combination of approaches are used to resolve the diagenetic paragenesis of the Farewell Formation for improved understanding of porosity development in the deeper parts (> 4500 mTVD) of the underexplored areas within the Taranaki Basin. More generally this work aims to contribute to improved understanding of the relationship between overpressure and reservoir quality in mature polyphase deformational basins and potential indicators of reservoir quality within them.

1.1. Geological setting

The Taranaki Basin covers approximately 100,000 km^2 underlying the shelf and continental slope west of central-western North Island (Fig. 1). It contains an Upper Cretaceous to Quaternary sedimentary fill up to 8 km thick, as described by King and Thrasher (1996). The basin comprises a relatively undeformed block (the Western Platform) and a heavily deformed area termed the Eastern Mobile Belt (King and Thrasher, 1996). The Eastern Mobile Belt contains significant shortening structures such as Taranaki Fault, where basement overthrusts Neogene and older formations, and the Manaia Anticline (Fig. 3). Both of these structures may have formed during the Late Eocene (Stagpoole and Nicol, 2008) and certainly by the Early Miocene (Kamp et al., 2014; King and Thrasher, 1996; Nelson et al., 1994). Kapuni Deep-1 was drilled into the Manaia Anticline (Fig. 3).

Fluvial sediments of the Palaeocene and Eocene section (Farewell, Kaimiro, and Mangahewa Formations) are the reservoirs for the Kupe, Kapuni, Mangahewa, and Turangi gas condensate fields (Figs. 1 and 2). Analysis of their reservoir sandstone beds reveals many of them to be overpressured, demonstrating the presence of distinct pressure zones (e.g. Webster et al., 2011). The primary cause of overpressure is interpreted to be disequilibrium compaction preserved in upper Eocene and Oligocene marine shales. In parts of the basin, hydrocarbon generation (and in particular cracking to gas at high maturities) is interpreted to contribute to the overpressures encountered in deeper portions of the basin (Webster and Adams, 1996; Webster et al., 2011). The poorly explored deeper and structurally compartmentalised sections of the basin, may yield potential for large dry-gas accumulations and good reservoir quality (Webster et al., 2011).

The sedimentary fill of Taranaki Basin records an early (84-57 Ma) phase of extension, which occurred concurrent with sea floor spreading in the Tasman Sea to the west. This extension has been attributed either to an intracontinental manifestation of a transform fault offsetting the spreading centre, or to a failed rift system (Strogen et al., 2017). From 52 Ma to ~40 Ma the basin was tectonically quiescent and passively subsiding, before the first manifestations of overprinting arising from development of the Australia-Pacific plate boundary through New Zealand, which may date from the Late Eocene (e.g. King and Thrasher, 1996).

Late Miocene inversion structures formed parallel to the major basin bounding Taranaki Fault, producing several anticlines that trap hydrocarbons in the Eocene Kapuni Group, which is comprised of a transgressive sequence of alternating sandstone, shale and coal beds, deposited under fluvial and fluvio-estuarine conditions (Voggenreiter, 1993). Thickening of strata against the Manaia fault (Figs. 1 and 3) identified by Stagpoole and Nicol (2008) suggests that displacement may have started during the Late Eocene. These structures contain the bulk of the proved hydrocarbon reserves in the major fields of Kapuni, Maui, Pohokura and Kupe South (Fig. 1). These inversion structures, which plunge to the north, formed through reactivation of Late Cretaceous-Palaeocene normal faults (Crowhurst et al., 2002). Farewell Formation crops out at Wharaiki Beach and the surrounding ridge in north-western South Island as a result of inversion on one of these types of faults. The eastern margin of North Taranaki Basin has been uplifted and eroded since the Early Pliocene as a result of doming of central North Island, preceding the 1.6 Ma outbreak of andesitic and silicic volcanism in Taupo Volcanic Zone (Armstrong and Chapman, 1999; Kamp et al., 2004). Turi-1 lies on the edge of this zone of uplift and experienced very little uplift and erosion, whereas about 1200 m of section has been eroded off lower parts of Mt Messenger Formation along the modern coast in North Taranaki Bight (Kamp et al., 2004). There has been ~300–400 m of exhumation of Late Pliocene section over the Kapuni Field during the past c.1 M y. (Kamp et al., 2004).

1.2. The Farewell formation

The Farewell Formation is a Palaeocene fluvial sandstone, extending

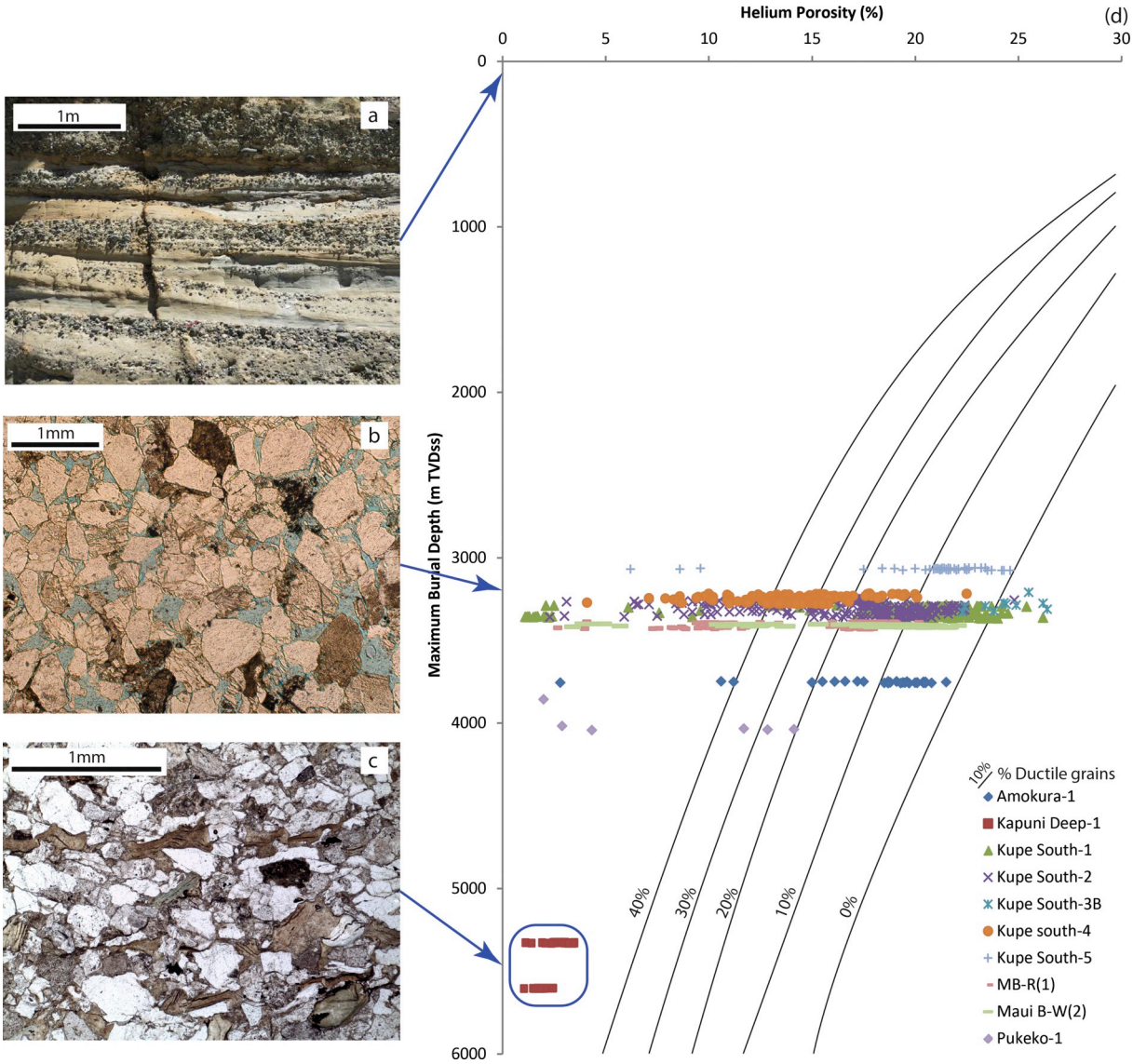

Fig. 4. a) Gravel conglomerate beds in Farewell Formation at Whariki Beach, Kahurangi National Park, Northwest Nelson (see Fig. 1 for location). b) Thin section micrograph of Farewell Formation at Kupe South-1 well displaying > 30% porosity (3100 mTVDss PPL). c) Thin section micrograph of Farewell Formation at Kapuni Deep-1 well displaying < 5% porosity (5335 mTVDss). d) Measured helium core plug porosity depth plot of Farewell Formation reservoirs (Compaction curves plotted for sandstones with varying ductile grain contents [0%, 10%, 20%, 30%, 40% from right to left]). Porosity-depth plot (after Trevena and Clark, 1986) compared to modelled trends. Porosity loss with depth has been modelled as a function of ductile sand content (after Atkinson and Bransby, 1978). No account has been taken of the effects of overpressure or the growth of mineral cements.

NE-SW across central parts of Taranaki Basin (Strogen, 2011, 2017). It was sourced from erosion of crystalline basement in north western South Island and structural highs within what is now Taranaki Basin, including granite batholiths of Cretaceous and Devonian age and Palaeozoic schists, quartzites and volcanics (Rattenbury et al., 1998). Farewell Formation has been interpreted as chiefly being deposited in fluvial, coastal plain and shore face to inner shelf environments (Strogen, 2011). To the north (down depositional dip) the formation inter-fingers with neritic to bathyal mudstone facies of Turi Formation, while to the north east it grades into shoreface facies deposited in a marginal marine environment, designated as F-sands (Strogen, 2011).

Exposures of Farewell Formation (Fig. 1) in coastal sections in Kahurangi National Park (NW Nelson) display multi-stacked multilateral sand bodies with abundant pebble-cobble grade beds (Fig. 4a) and coal seams of up to 2 m thick. These coal seams and others of Late Cretaceous age are postulated to be the source of oil and gas in productive fields within Taranaki Basin (Killops et al., 1998; King and Thrasher, 1996).

1.2.1. Reservoir stratigraphy

Farewell Formation forms the primary reservoir for the Kupe South Field in southern Taranaki Basin and its diagenetic history has previously been investigated by Martin et al. (1994). Farewell Formation at Kupe South has been subdivided into four seismically defined (A-D sands) intervals by Schmidt and Robinson (1989). The lower two of these (A and B sands) are hydrocarbon-bearing and have been further classified into upper and lower sands by Martin et al. (1994) based on petrological differences. The lower/B sand porosity and permeability is controlled predominantly by grain size and the presence of chlorite/smectite, whereas the upper/A sand is controlled by kaolinite content.

The Farewell Formation in Kupe Field is close to 90% net:gross, while mud log cuttings collected from the Farewell interval at Kapuni Deep-1 indicate a lower net:gross of c.80%, though some cored sections display higher values (Fig. 4). The lack of core collected in the Farewell Formation on the Taranaki Peninsula does not allow for the identification of specific units noted in the Kupe Field. Oil shows were encountered between 5446 and 5520 m in Kapuni Deep-1, and fractures in

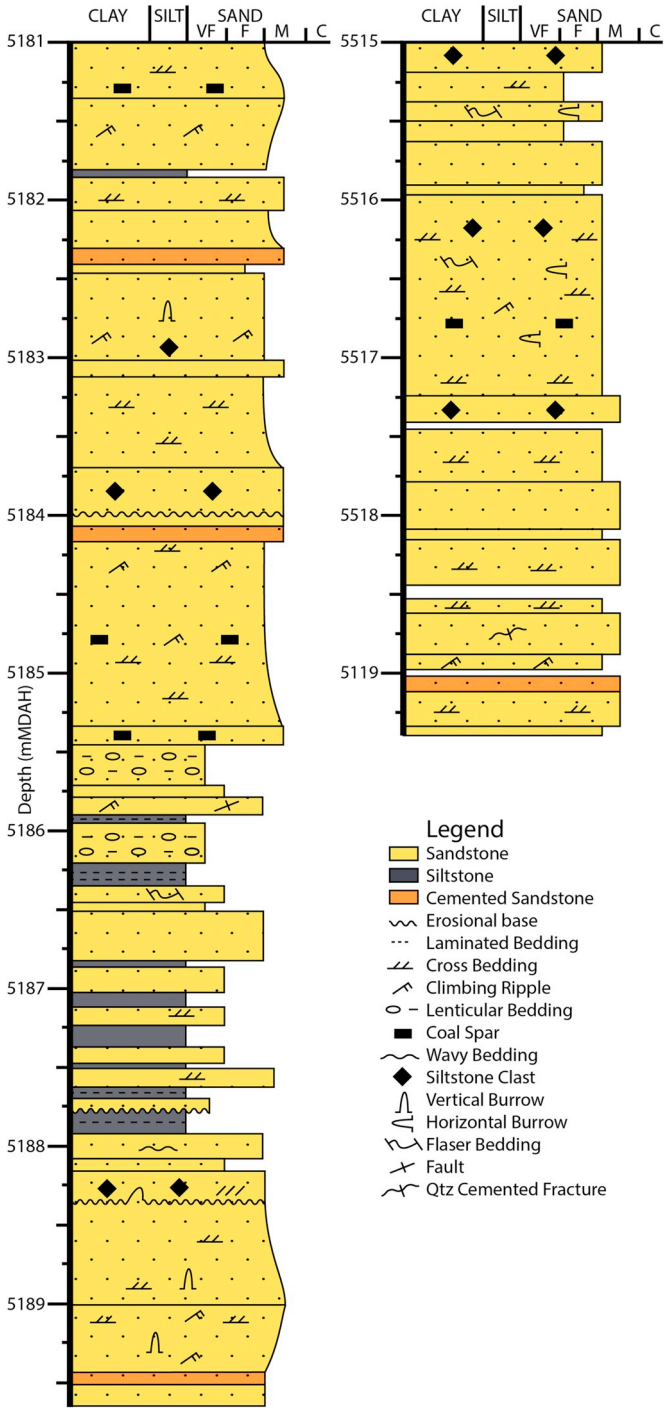

Fig. 5. Sedimentary log through both of the Farewell Formation cores from Kapuni Deep-(Burn et al., 1995; STOS, 1984).

core at this depth display good yellow-green fluorescence and dark brown oil staining (STOS, 1984). Core analysis results showed the reservoir to be tight (0.1 mD), which together with dipmeter data from the cored interval suggests that shows are associated with fractures. Oil charged micro-fractures have apertures of up to 1.5 mm. Source rock intervals in Kapuni Deep-1 are confined to interbedded coals within the Farewell Formation, which are vitrinite rich and gas prone, but modelling has shown them to be mature for oil since c.2 Ma (Higgs et al., 2013).

1.3. Overpressure generation, preservation and dissipation

Overpressure in clastic sedimentary basins is created by two main groups of mechanisms: (1) stress applied to a compressible rock (disequilibrium compaction, lateral compression); and (2) fluid expansion and/or increase in fluid volume (through hydrocarbon cracking, gas generation and load transfer) (Lahann and Swarbrick, 2011; Swarbrick et al., 2002). Excess pore pressure is preserved by the presence of an effective top seal and lateral barriers to flow which can be both stratigraphic and structural. Both sealing mechanisms can be found in the Taranaki Basin, for example the Oligocene Tangaroa Formation is an overpessured basin floor fan is encased in the Turi Formation, a massive marine mudstone (Fig. 2). Structural compartmentalisation can also be found in the form of sealing faults across the Taranaki basin, as seen in the McKee Field of the Tarata thrust Zone on the basin's Eastern Margin (Fig. 2). The Field is comprised of a series of independent thrusted fault blocks, some of which are in pressure communication, while others are confined by sealing faults so act as isolated pressure cells that restrict flow across the field.

Overpressure can be lost through top seal failure; though pressures within the Taranaki Basin are generally safely below the minimum stress gradient at the present day, so seal failure by overpressure-driven hydraulic fracturing is unlikely to be a significant risk across much of the basin (Darby, 2002). Fluid pressure can be dissipated through episodic fault plane leakage, which has been demonstrated in Taranaki Basin (Webster et al., 2011).

Basin plumbing is a 3D system, involving lateral fluid flow in the form of lateral drainage where pore fluids move from a higher to lower overpressure facilitated faults or/and fractures and lateral continuous reservoirs packages (O'Connor and Swarbrick, 2008). Such continuous connected reservoirs are present in the Manaia Graben and southern Taranaki Basin.

1.4. Pore pressure distribution

The polyphase nature of the basin evolution has led to a complex pore pressure history, producing a significant variation in present day vertical and lateral distribution of overpressure. Cretaceous to Early Miocene formations are either normally pressured (near or at hydrostatic) or significantly overpressured (> 1500 psi/10 MPa) at the same depth in different parts of the basin, as shown in the cross section in Fig. 3.

Webster et al. (2011) designated three semi-stratigraphically separated pressure cells in Taranaki Basin: a near-hydrostatic interval (Zone A) which extends from surface to varying depths in different parts of the basin; a generally underlying overpressured interval (Zone B) of approximately 1200 psi (8.2 MPa), which extends from c.1900 m to c.4000 m; and a third interval (Zone C) of > 2000 psi (13.8 MPa), which directly underlays zones A & B in different parts of the basin. The Oligocene to early Miocene Otaraoa Formation, a bathyal calcareous mudstone acts as the principal top seal between hydrostatic Zone A, and deeper variably overpessured zones (Figs. 2 and 3). The Otaraoa and underlying massive marine mudstone of the Turi Formation are considered to be the formations where overpressure (low vertical effective stress) is generated in the basin, through the mechanism of disequilibrium compaction (Webster et al., 2011).

2. Methodology

2.1. Sampling

In Kapuni Deep-1, approximately 1700 m of Farewell Formation was encountered and two conventional cores (Fig. 5) were cut at 5181-89 & 5515–19.4 mMDAH (measured depth along hole). Seventeen core samples were collected from sandstone beds in the upper (11) and lower core (6) of Kapuni Deep-1. The samples were predominantly

taken from sections of clean sandstone with a lack of shale or coal laminae. Thin sections of these were produced for transmitted light microscopy, SEM and QEMSCAN (Quantitative Evaluation of Minerals by SCANning electron microscopy) analysis; as well as fluid inclusion wafers and rock chips for x-ray diffraction analysis. Twelve polished thin sections were obtained from the New Zealand Petroleum & Minerals collection. Petrophysical wireline data acquired over the cored intervals are representative of the Farewell Formation below 5000 mTVDgl (Total Vertical Depth below ground level).

2.2. Petrographic analysis

Samples were analysed using transmitted-light microscopy on impregnated thin sections and modal analysis was undertaken on all samples to ascertain mineralogy (300 counts per section). The resulting data were used to calculate intergranular volume (IGV) (Paxton et al., 2002), porosity loss through mechanical compaction (COPL) and porosity loss by cementation (CEPL) (Lundegard, 1992):

$$COPL = P_i - \left(\frac{(100 - P_i)P_{mc}}{100 - P_{mc}}\right)$$

$$CEPL = (P_i - COPL)\left(\frac{C}{P_{mc}}\right)$$

where Pi is the initial or depositional porosity and Pmc is the intergranular volume or minus-cement porosity calculated by subtracting the total cement volume (C) from the total optical primary porosity (Po). The calculated COPL and CEPL are accurate if three conditions are met. First, the assumed initial porosity (Pi) must be correct. Second, the amount of cement derived by local grain dissolution must be negligible or known. And third, the amount of framework mass exported by grain dissolution must be negligible or known (Lundegard, 1992). The initial or depositional porosity of Farewell Formation has been estimated as 42% (Pryor, 1973).

All thin sections were highly polished to 30 μm and coated with 30 nm of carbon before analysis by a Hitachi SU-70 field emission scanning electron microscope (SEM) equipped with an energy-dispersive detector (EDS). Backscatter scanning electron microscopy of thin sections was conducted at acceleration voltages of 15 kV with a beam current of 0.6 nA. The SEM-EDS assembly was used for rapid identification of chemical species and their orientation in the sample. Scanning electron microscopy was undertaken on selected samples, providing additional information on the pore-system geometry, authigenic mineralogy, and paragenetic relationships. The analysis was undertaken on gold palladium coated, freshly broken samples glued onto aluminium stubs with silver paint. Cathodoluminescence analysis was undertaken on selected thin sections with visible macro quartz overgrowths using a Gata MonoCL system with a panchromatic imaging mode operated at 15 kV. QEMSCAN data were collected on one representative sample depth (5518.1 mMDAH) from the lower core to supplement XRD (x-ray diffraction), scanning electron microscopy and modal analysis.

Microthermometry was conducted on doubly polished detached wafers to determine the conditions of cementation and evidence for formation water salinity. Fragments were cut from doubly polished rock wafers. The wafers were firstly checked under incident UV on a petrographic microscope to determine which ones contained petroleum inclusions, as well as under transmitted light to determine the distribution of both aqueous and non-aqueous fluid inclusions for subsequent analyses. The fluid inclusion and x-ray diffraction analyses were undertaken following the methodology as outlined in Stricker et al. (2018).

2.3. One dimensional burial history modelling

Pore pressure evolution within the stratigraphy intersected by Kapuni Deep-1 was modelled in one dimension using Schlumberger's PetroMod (V. 2015) software. One-dimensional modelling provides a good insight into overpressure build-up by disequilibrium compaction, which is regarded as the principal driver in Taranaki Basin (Webster et al., 2011). PetroMod is based on a forward modelling approach to calculate the geological evolution of a basin from its burial history (Hantschel and Kauerauf, 2009). However, the models do not include other mechanisms for generating excess pore pressure, such as hydrocarbon cracking, gas generation or load transfer (Lahann and Swarbrick, 2011) and are only able to account for vertical stress'. 1D modelling will also not show the potential discrepancies in overpressure between reservoir and shales caused by lateral fluid flow, but this can be calibrated using measured reservoir pressure data where available. The generation and dissipation of pore pressure is a 3D process, which is not captured in a 1D system. Fluid flow in the form of lateral drainage, lateral transfer and fault related flow have been identified in the Taranaki (Webster et al., 2011), and must be taken into consideration when interpreting modelling results.

The burial model uses present-day well stratigraphy provided by the Kapuni Field operator, Shell Todd Oilfield Services and lithologies created from mud log cuttings data in the well completion report (STOS, 1984). Heat flow has been estimated after Funnell et al. (1996), uplift from Armstrong et al. (1998) and palaeo-water depth from King and Thrasher (1996). The model was calibrated against corrected bottom hole data for the Kapuni Field (Rob Funnel pers. comm. 2017), measured formation pressures and helium porosity (Figs. 6c and 7b) (STOS, 1984).

3. Results

3.1. Farewell sandstone composition

The Farewell Formation at Kapuni Deep can be characterised as a sub-arkosic arenite (Figs. 7a and 8c) with abundant quartz (av. 47%) and feldspar (av. 21%); rock fragments of granite, schist, arenite and volcanics, make up av. 5% of the grains (Table 1). The detrital grains range in size from very fine to fine sand and are predominately angular to sub-angular, with minor intervals comprised of medium sand. There are calcite cemented zones up to 10 cm thick (Fig. 5) and primary pore filling authigenic clay minerals that form between 3 and 10% of the rock (Table 1). Detrital micas are present in most sections varying between 1 and 6% in abundance (Table 1), with high percentages occurring in shale rich sections (Fig. 8c). Micas can vary between being undeformed to heavily deformed. Detrital mud clasts are most prevalent in shale rich samples forming up to 8% abundance (Table 1). QEMSCAN (Fig. 8c and d) and SEM-EDS analyses identified the presence of detrital titanium oxide (1–3%). Significant replacement of detrital grains by clay and carbonate cement occurs in all samples. Rare hydrocarbon streaks are present within primary porosity.

Core logs (Fig. 5) and thin sections demonstrate that sandstone beds are interbedded with thin siltstone, shale and coal beds at millimetre to tens of centimetre scale, possibly representing a marsh or floodplain within a palaeo braided river system (Strogen, 2011). Siltstone clasts up to 5 cm in diameter are common within sandstone beds; as are sandstone lenticles within shale horizons. Many of the shale horizons have convolute bedding, which could be attributed to sediment loading, slumping, liquefaction or disruption by plant roots.

3.1.1. Compaction

Concavo-convex and quartz-to-quartz long grain contacts are common in all sections, which are indicative of significant mechanical compaction. The COPL-CEPL results, shown in Fig. 7e, indicate that mechanical compaction is the driver of porosity loss in both cored

sections, leading to minimal primary porosity (Figs. 4c, 7c and 8a) and low IGVs (Fig. 7d).

3.1.2. Authigenic clay minerals

Authigenic kaolinite occurs as variably sized plates and books, filling pores and replacing partially or fully dissolved detrital grains (Fig. 9a), and forms aggregates up to the size of detrital grains (Fig. 9c). The micro-porosity within pore filling clay aggregates, predominantly kaolinite, is often stained black due to hydrocarbons. Clay coatings could not be distinguished in reflected light, but SEM, SEM-EDS and QEMSCAN analyses identified sporadic thin chlorite alongside mixed layer Illite/smectite coats (Table 3). Illite bridges open pores and secondary porosity in dissolved calcite cement cavities (Fig. 9b). Sanadine (sourced from volcanic fragments) is the feldspar most susceptible to dissolution, but all feldspars have been affected (Smale et al., 1999). X-ray diffraction data show there to be an inverse relationship between Kaolinite and feldspar abundance (Table 2).

3.1.3. Carbonate cement

Calcite cement is confined to thin sporadic intervals, as shown in the core log for Kapuni Deep-1 (Fig. 5) and bulk rock XRD results (Table 2). Thin section (Fig. 8b) observations show the cement to be coarsely crystalline sparite, that can enclose all forms of authigenic clay and fill secondary grain dissolution and fracture porosity (Fig. 9b). QEMSCAN analyses (Fig. 8c and d) have shown the calcite cement to be sporadically developed even within these carbonate rich zones. Modal analysis from a single thin section has shown calcite can contribute up to 40% of the rock (Table 1) found in primary pores and replacing both dissolved quartz (Fig. 9b) and feldspars. XRD analyse from a single carbonate cemented sample shows calcite to form 33% of the bulk rock (Table 2). The upper Kapuni Deep-1 core displays significantly less calcite cement with an average abundance of 0.9% compared with 7.0% in the lower core (Table 1), which could be explained through the presence of corrosion surfaces on euhedral quartz grains (Collen, 1988), which is indicative of carbonate dissolution. Carbonate cement in Farewell Formation in the Kupe South Field incompletely replaces feldspars, rock fragments and micas, ranging from 10% to 55% of the bulk rock (Martin et al., 1994).

Carbon isotope analysis of carbonate cements sampled from overlying Kapuni Group reservoirs, display enrichment in isotopically light carbon (Higgs et al., 2013), which is sourced through thermal maturation of organic material (Franks and Forester, 1984), meaning that the carbonate precipitated from organic CO_2 via the breakdown of hydrocarbons.

3.1.4. Quartz cementation

Pressure dissolution and stylolitisation of quartz grains has been identified in reflected light microscopy (Fig. 8a) and in backscatter SEM images (Fig. 9a and c), prompting analysis by cathodoluminescence of selected samples to investigate the extent of silica cementation. Rare poorly developed and often interlocking anhedral quartz overgrowths (Fig. 9e and f) and very rare feldspar overgrowths are present. Macro-quartz that fills fractures in quartz grains (Fig. 9e) displays similar fluorescence to the overgrowths, which is suggestive of equivalence. Diagenetic micro-quartz is also present as rims on detrital quartz grains and as overgrowths (Fig. 9e and f).

3.1.5. Porosity

Core analysis results (Fig. 7c) show helium reservoir porosities range between 1 and 4.5%. Very limited intra-granular porosity can be identified in reflected light (Fig. 8a). The low intergranular volumes are supported by the measured porosity values, as helium techniques measure total porosity, which includes micro-porosity within clay cement. The final present day basin modelling derived porosity of c. 8% (Fig. 6c) is slightly higher than the measured helium porosities, the further loss could attributed to pervasive authigenic clays and calcite filling pores. Locally, secondary porosity is associated with dissolution of feldspars, quartz and of calcite cement.

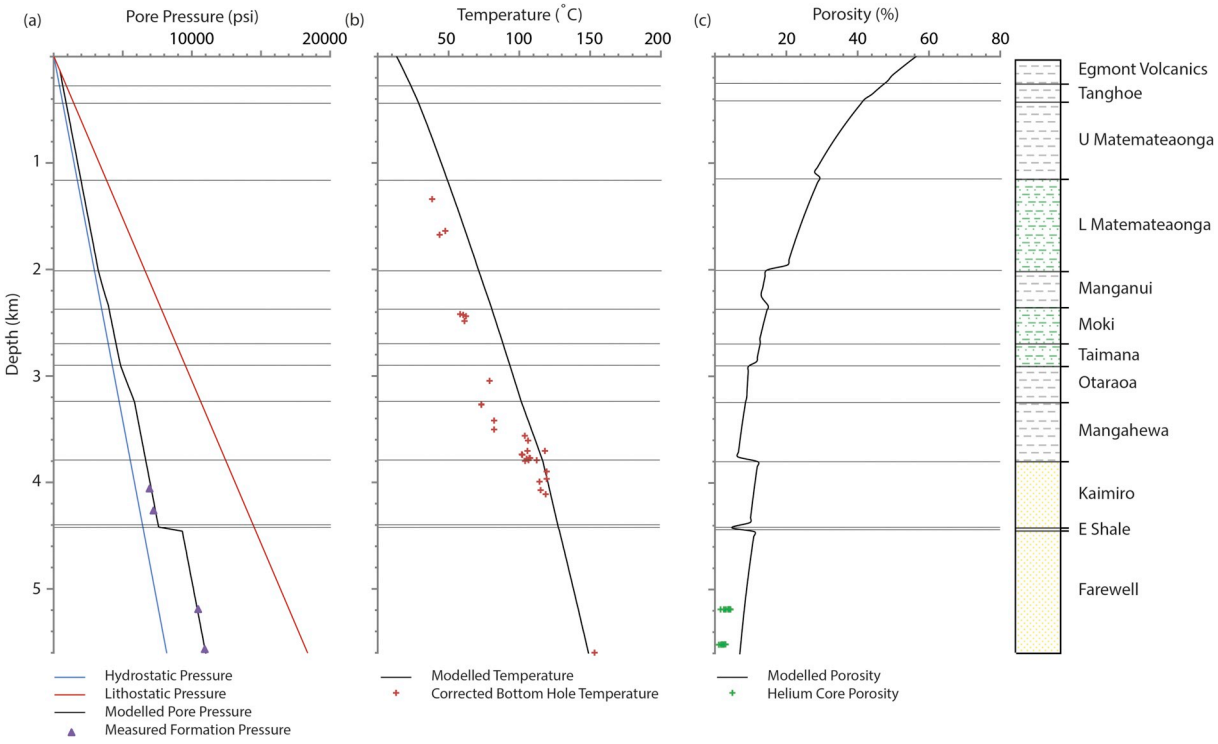

Fig. 6. Calibration data for 1D basin model for Kapuni Deep-1 well. a) Plot of modelled and measured formation pressure gradient against depth. b) Plot of modelled formation temperature and corrected bottom hole temperature against depth. c) Plot of modelled porosity and measured helium core porosity from the Farewell Formation.

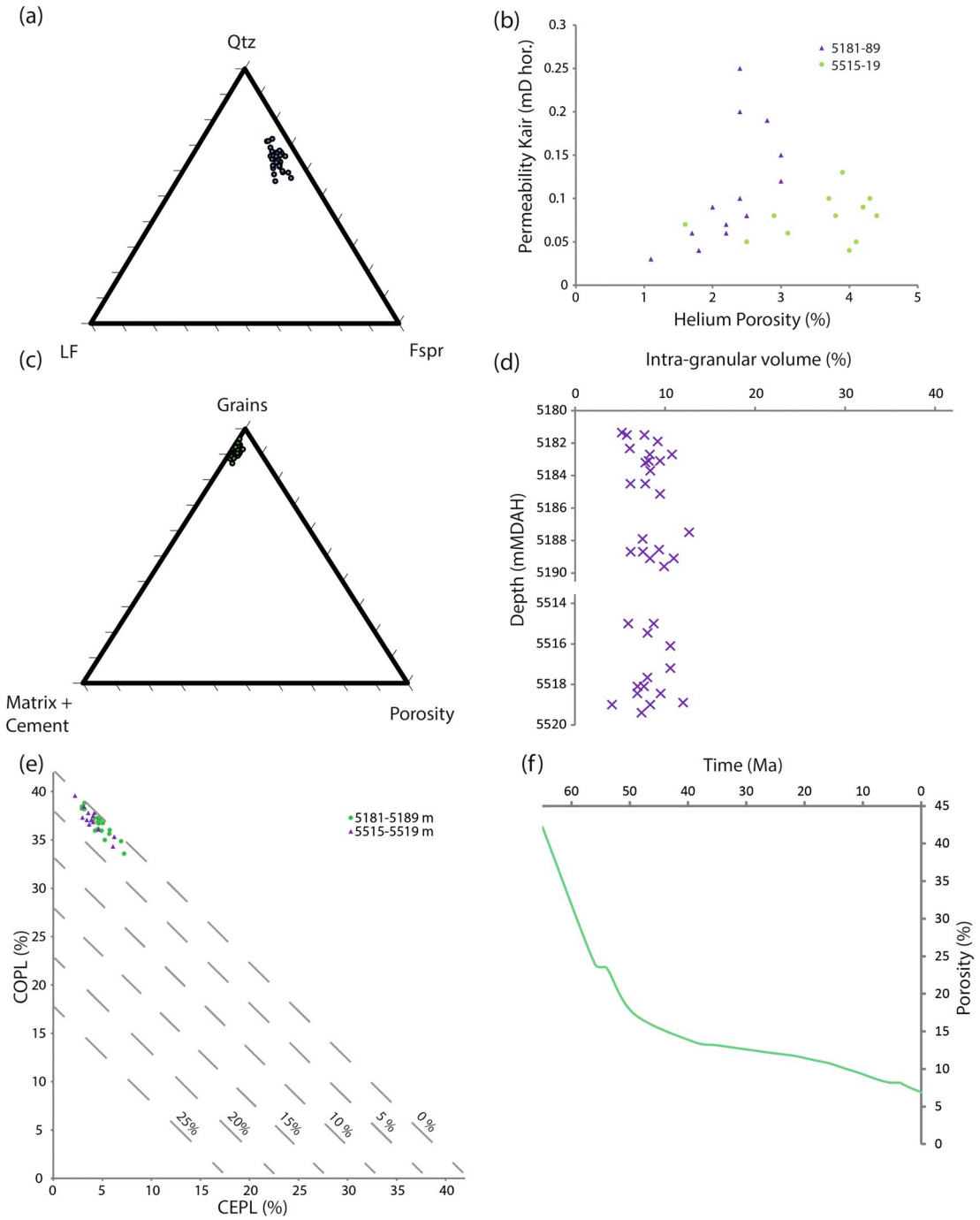

Fig. 7. a) Ternary plot of present day composition of the Farewell Formation at Kapuni Deep-1 from point count data (Table: 1). b) Measured porosity permeability cross-plot from core analysis data of the Farewell Formation at Kapuni Deep-1 [green circles 5181–5189 mMDAH and purple triangles 5515–5519 mMDAH] (STOS, 1984). c) Ternary plot displaying grains: matrix: porosity ratio of Farewell Formation data at Kapuni Deep-1 from point count measurements. d) Plot of inter granular volume variation with depth in the Farewell Formation at Kapuni Deep-1. e) Compactional (COPL) and cementational (CEPL) porosity loss for Kapuni Deep-1 [green circles 5181–5189 mMDAH and purple triangles 5515–5519 mMDAH] with remaining sample porosity (dashed lines). COPL and CEPL calculated after (Lundegard, 1992). f) Plot of modelled porosity of the lower core (c. 5500 mTVDgl) of the Farewell Formation at Kapuni Deep-1 against time. (For interpretation of the references to colour in this figure legend, the reader is referred to the Web version of this article.)

3.1.6. *Fluid inclusions*

Very few definitively diagenetic pore-occluding quartz overgrowths were identified and of these only a small proportion display fluid inclusions. Oil inclusions that are present possess semi-opaque to opaque backgrounds in transmitted light, which prevents microthermometry and hence no other aqueous inclusions could be located in conclusively diagenetic phases, limiting analyses to both aqueous and mixed hydrocarbon aqueous phase inclusions in quartz micro-fracture fills (Table 4). The sediments are first cycle derived from granitic and metamorphic basement in the North West Nelson area, meaning that oil and micro-fracturing must be related to the present basin fill (as opposed to inherited from a previous sedimentary sequence that was sourced to the basin). Results from samples prepared from both of the Kapuni Deep-1 cores display virtually identical fluid inclusion properties, suggesting the presence of an undersaturated oil (hence the disparity between aqueous and oil homogeneity temperatures) trapped at

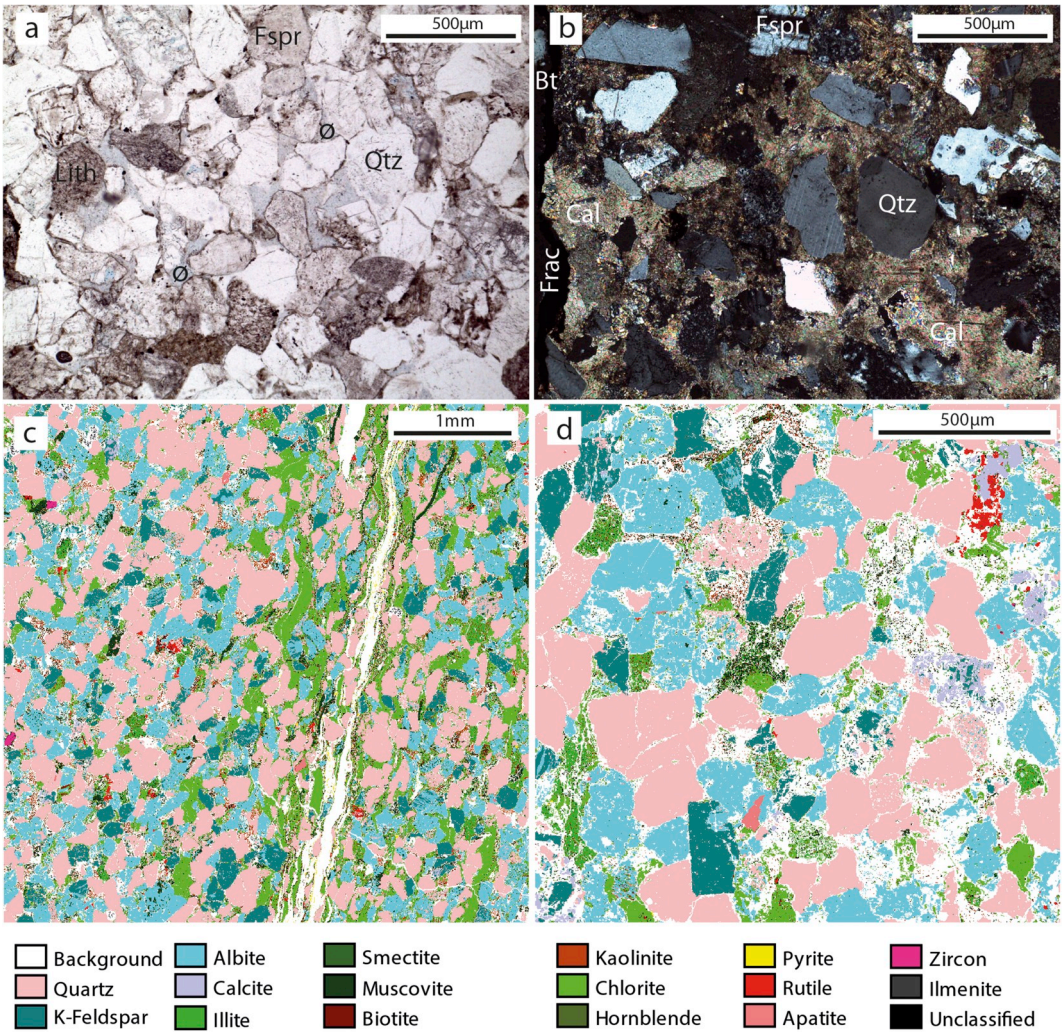

Fig. 8. a) Thin section micrograph (5189.1 mMDAH): limited visible inter-granular porosity, texturally immaturity and concavo-convex sutured grain contacts. b) Thin section micrograph (5518.9 mMDAH): early calcite cement has created grain framework reducing grain-grain contacts (Lith = lithic fragments; Fspr = feldspar; Qtz = quartz; Frac = fracture; Bt = bitumen; cal = calcite). c) QEMSCAN image (5518.1 mMADAH): bitumen filled fracture with clay smear and mica grains. d) QEMSCAN image (5518.1 mMADAH): higher resolution scan displaying sporadic carbonate cement, degraded feldspar grains and pore filling clay cement: primarily kaolinite, mixed layer Illite smectite and chlorite.

105–125 °C (av. 110 °C), in waters of brackish salinity (Table 4). Temperatures from burial history modelling suggests that inclusions where trapped between 6 and 4 Ma. The oil inclusions identified in macro-quartz overgrowths display a reasonably consistent fluorescence colour throughout (Table 5), indicating little liquid compositional variation, as reflected in the relatively narrow spread of spectrometric API gravity estimates of 30 ± 5 °C ('moderate'). They are, however, in low abundance, which, if drawn from the same petroleum column, suggests low permeability or poor generation at the time of trapping.

3.2. Vertical pressure distribution

Offset well data (Stratford-1, Fig. 1) from the Manaia Graben indicate that the Early Miocene to Pliocene stratigraphic section in Kapuni Deep-1 is very likely to be near to, or at, hydrostatic pressure. Offset wells have been used to calculate a basin wide hydrostatic gradient of 0.434 psi/ft (0.01 MPa/m). The wireline signatures of the sonic, density and resistivity logs display clear regressions from top Moki Formation downwards, which is an indication of under-compaction and the existence of overpressure (Fig. 10), primarily within the Oligocene Otaraoa Formation. Shale pressures were calculated using the equivalent depth method (Hottmann and Johnson, 1965), and also suggest that the Otaraoa Formation is overpressured (Fig. 10). The mud log through the Oligocene to Mid-Miocene section indicates close to 100% fine-grained lithology and therefore low permeability; inhibiting the inflow of pore water into the borehole, so any overpressure in the shales is therefore not reflected in the mudweight.

RFT measurements collected at Kapuni Deep-1 in the Middle Eocene Kaimiro Formation gave an average pore pressure of 6939 psia/48 MPa (1443 psia/10 MPa overpressure), which is consistent with the virgin pressure of the K3E reservoir interval recorded elsewhere in the Kapuni Field. The lack of influence from production within the Kaimiro Formation implies that there is no pressure communication, indicating lateral compartmentalisation on a production timescale. This overpressure is also in line with measurements taken in the overlying Mangahewa Formation recorded elsewhere in the field, indicating that the intervening Omata Member of Turi Formation is not acting as a vertical seal at Kapuni Deep-1 (Webster et al., 2011).

In Kapuni Deep-1 a constant mudweight of 10.4 ppg/1246.2 kgm^2 was maintained through the Eocene and into the Palaeocene, until two drilling breaks occurred at 5155 and 5171 mTVDgl, which both resulted in water influxes. Drill mudweight and shut-in drill pipe pressures were used to calculate a reservoir overpressure of 3393 psi/23.4 MPa from the second deeper kick, indicating that the well was drilled 1513 psi/

Table 1
Modal point counting summary.

Depth		Point Count (300)														
(mMDAH)	(mTVDgl)	Quartz (%)	Lithics (%)	Feldspar (%)	Fracture Porosity (%)	Primary carbonate cement (%)	Replaced carbonate cement (%)	Unknown carbonate cement (%)	Mud clasts (%)	Hydrocarbon streak (%)	Mica (%)	Primary clay cement (%)	Replacement Clay cement (%)	Unkonwn Clay cement (%)	Secondary porosity (%)	IGV (%)
5181.35	5161.04	53.3	3.7	22.3			0.3		1.3		0.3	5.0	10.0	3.3	0.3	5.2
5181.50	5161.19	54.3	5.0	21.7			0.3		0.7		1.3	7.7	8.3	0.7		7.7
5181.50	5161.19	52.3	4.0	22.0			1.0		1.7	1.0	1.0	4.7	10.7	1.7		5.8
5181.90	5161.59	47.3	8.0	22.3	1.0				1.3	1.0		7.0	10.0	1.3	0.7	9.2
5182.33	5162.01	52.3	7.0	20.3		0.3	1.7	0.3	1.3	1.3	1.3	4.3	8.7	0.7	0.3	6.1
5182.70	5162.38	49.0	5.3	22.7		0.3		0.3	0.7	1.0	0.3	6.7	10.3	2.3	1.0	8.3
5182.70	5162.38	54.3	5.3	16.3	0.7	0.3	2.0		2.0	2.0		7.7	8.3	1.0		10.8
5183.10	5162.78	52.7	3.7	22.7					2.3	1.0	1.3	7.0	7.0	2.0	0.3	8.2
5183.10	5162.78	49.0	3.0	22.7					3.3	2.7	0.7	6.3	7.7	4.3	0.3	9.4
5183.20	5162.88	50.3	5.3	23.7					2.0	1.3	1.0	6.3	8.0	2.0		7.8
5183.70	5163.38	47.0	5.0	20.0	0.3		0.3		1.7	0.7	1.3	7.0	12.3	4.3		8.4
5184.50	5164.17	48.3	6.0	23.3		0.7	1.0	0.3	2.7	1.0	0.3	4.3	9.7	1.3	1.0	6.2
5184.50	5164.17	44.3	5.0	28.3		1.0	1.0		2.3	1.3	1.0	5.3	8.7	1.0	0.7	7.8
5185.14	5164.81	49.3	5.0	19.7	1.0		1.3		2.3	0.7	1.0	7.3	7.7	3.3	1.3	9.4
5187.50	5167.16	40.3	3.7	12.3					5.0	1.7	5.7	10.0	13.3	7.0	1.0	12.7
5187.90	5167.56	52.0	3.7	21.0			1.3	0.3	3.0		1.3	7.3	8.0	1.7	0.3	7.5
5188.56	5168.22	46.0	6.3	19.0			0.3		2.7	0.3	0.7	8.7	12.3	1.7	2.0	9.3
5188.70	5168.36	50.7	6.0	20.3		0.7	0.3		2.0	0.3	0.3	6.3	10.3	0.3	2.3	7.5
5188.70	5168.36	50.7	4.7	20.7	0.7	0.3	1.0		4.3	0.3	0.7	4.7	9.0	2.3	0.7	6.2
5189.10	5168.76	41.0	5.0	20.0					8.0	0.3	3.7	10.3	9.0	1.7	1.0	11.0
5189.10	5168.76	38.3	8.3	22.0					3.7	0.3	3.7	7.7	12.0	2.7	1.3	8.3
5189.60	5169.25	44.7	6.0	24.7			2.0		1.3	1.0	0.3	8.7	9.0	1.7	0.7	9.9
5515.00	5492.78	46.3	6.0	23.0	2.3	0.3	2.7		3.3	0.3		5.3	8.3	1.7	0.3	8.5
5515.00	5492.78	47.0	9.0	24.3			2.0	0.3	3.3	0.7		5.0	7.0	1.3		5.8
5515.46	5493.23	45.7	6.0	24.7			1.3		3.0	1.7	1.0	6.0	8.3	1.0	1.3	7.8
5516.10	5493.87	41.7	5.3	20.3		2.0	3.3	0.3	3.3	0.7	0.7	7.3	12.3	2.0	0.7	10.3
5517.20	5494.96	47.0	5.0	19.7		2.7	3.7	0.3	3.0	0.7	0.7	6.7	8.0	2.0	0.7	10.3
5517.66	5495.42	44.0	7.0	20.0	0.7				6.0	1.7	2.0	5.3	11.3	1.7	0.3	7.8
5518.10	5495.85	48.3	5.0	16.7	0.3	1.0	1.7		3.7	0.7	1.0	4.7	15.7	1.0	0.3	6.8
5518.10	5495.85	45.7	5.0	17.0			1.7		2.0	2.7	0.7	4.7	19.0	1.0	0.7	7.5
5518.45	5496.20	44.0	4.7	25.7		1.0	3.3		3.3		1.0	5.7	10.3	0.7	0.3	6.7
5518.45	5496.20	42.3	5.3	19.0		1.7	7.0	0.7	2.7	2.0	1.0	5.3	11.0	1.7	0.3	9.2
5518.90	5496.65	29.7	3.3	13.3	1.0	7.7	34.0	3.0	4.3	1.3	1.0	1.3				11.7
5519.00	5496.75	50.0	3.3	15.7			4.7		4.0	1.7	2.0	6.3	10.7	1.7		8.1
5519.00	5496.75	47.7	4.0	20.7		0.3	4.7		4.0	0.3	2.3	3.3	12.3	0.3		4.0
5519.40	5497.14	39.0	5.0	17.7		2.0	16.7	1.3	1.7	0.7	1.0	4.3	9.3	1.3		7.2

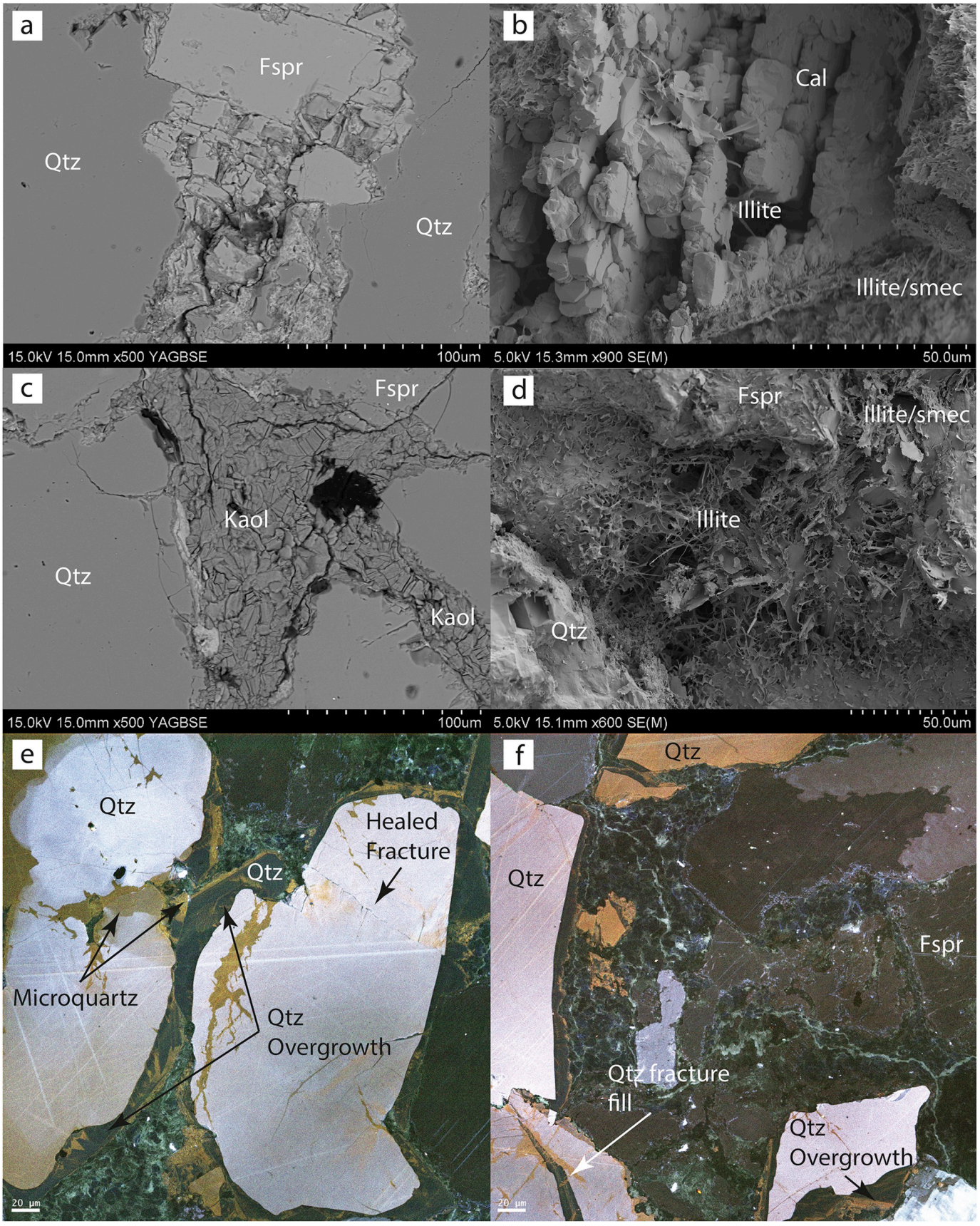

(caption on next page)

Fig. 9. a) BSEM image (5518.1 mMDAH): heavily degraded feldspar grain and sutured contacts. b) SEM image (5187.9 mMDAH): calcite crystal that has been partially dissolved and bridged by Illite. c) BSEM image (5518.1 mMDAH): undercompacted pore filling kaolinite books. d) SEM image (5518.9 mMDAH): a pore lined by mixed layer illite/smectite and bridged by illite crystals; e) SEM-CL panchromatic false colour image (5183.7 mMDAH): displaying quartz overgrowths, micro-quartz and a healed fracture. f) SEM-CL false colour image (5183.7 mMDAH): minor quartz overgrowths and a quartz filled fracture within detrital quartz grain (Qtz = quartz; Fspr = feldspar; Cal = calcite; Kaol = kaolinite; smec = smectite). (For interpretation of the references to colour in this figure legend, the reader is referred to the Web version of this article.)

10.4 MPa underbalance.

3.3. Burial history modelling and pore pressure evolution

Deposition of the Farewell Formation began during the Early Palaeocene on a coastal plain as indicated by the presence of coal, coarse grained sandstones and pebble conglomerates of fluvial origin (Fig. 4a). These deposits were rapidly buried (150 m/M.y.) during the Palaeocene to Early Eocene during waning basin extension (Fig. 11). Mud log cuttings indicate that the c.3 km thick Palaeocene to Middle Eocene succession in Kapuni Deep-1 is almost entirely comprised of very fine to medium sandstone. The formation of overpressure is dependent on the presence of fine-grained lithologies where excess pressure is generated through disequilibrium compaction, as well as to act as seal to the pressure that has been transferred into reservoir/more permeable units. The 1D basin modelling shows that these sand rich sediments allowed vertical dewatering, leading to maintenance of close to hydrostatic conditions (Fig. 11a).

The rate of subsidence and sediment accumulation reduced during the Middle Eocene to Early Oligocene interval during post-extension thermal contraction. Slow rates of burial did not lead to the generation of any significant overpressure. Water depths across the whole of Taranaki Basin increased during the Oligocene, leading to the deposition of the 200 m thick Otoraoa Formation as a bathyal marine calcareous mudstone. The Otoraoa Formation is considered to have undergone limited initial compaction due to slow subsidence rates, but was subsequently buried by several km of terrigenous Miocene mudstone (e.g. Manganui Formation). This allowed for limited dewatering, leading to the onset and generation of small amounts (c 400 psi) of overpressure through disequilibrium compaction from the Miocene onwards (Fig. 11b).

By the Late Miocene (c. 10 Ma) the rate of burial, particularly in southern and central parts of Taranaki Basin slowed and was followed by changes in the sense of displacement on prior normal faults, the associated development of anticlinal inversion structures and widespread uplift of southern Taranaki Basin (Crowhurst et al., 2002; Kamp and Green, 1990). Manaia Anticline in southern Taranaki Peninsula, which carries the Kapuni Field (Higgs et al., 2013), also developed at this time with ~300 m of erosion of Late Miocene section along the axis of the anticline (Armstrong et al., 1998). Horizontal stress enforced through the shortening may have led to increase in pore pressure as seen in the New Zealand's East Coast Basin (Burgreen-Chan et al., 2016). Though due to the limitations of 1D basin model this cannot be tested, though by the Pliocene, movement on the Taranaki fault had ceased, meaning any excess pore pressure generated by horizontal stress would have started to dissipate, during the current extensional phase of the Taranaki Basin (Rajabi et al., 2016). Also, the erosion over the Kapuni Field will have enabled some pressure dissipation (Fig. 11b).

There was renewed subsidence and high sedimentation rates (620 m/M.y.) across southern Taranaki Peninsula and offshore immediately to the south during the Pliocene. This involved Kiore Formation and Matemateaonga Formation, which accumulated in shelfal environments in Taranaki Peninsula, followed by accumulation of mid Pliocene Tangahoe Mudstone in upper bathyal environments and Late Pliocene Whenuakura Subgroup in shelfal environments (Kamp et al., 2004). The driving mechanism for the development of late overpressure in Palaeogene section below Oligocene Otaraoa Formation seal is considered to be the rapid phase of Late Miocene and Pliocene burial in central to southern parts of the Taranaki Peninsula parts of Taranaki Basin.

3.4. Diagenetic paragenesis

Diagenesis will have initiated during shallow burial with pore-filling carbonate cementation, supported by the lack of grain-grain point contacts in heavily cemented section sampled (Fig. 8b). Calcite cement in Farewell Formation at Kapuni-14 (4309 mTVDgl) has a $\delta^{18}O$ value of −2.6‰, corresponding to precipitation from seawater at 28 °C (Smale et al., 1999). Dolomite sampled in the same horizon interval precipitated at 60 °C ($\delta^{18}O$ −6.0 ‰) and calcite from the deeper cored section of Kapuni Deep-1 produced an $\delta^{18}O$ value of −15.3 ‰, corresponding to precipitation from sea water at approximately 121 °C (Smale et al., 1999). Although there are few oxygen isotope analyses, these data suggest that carbonate cementation occurred over an extended interval through the Miocene and Pliocene during burial of Farewell Formation.

The onset of feldspar and mica degradation will have occurred during burial, contemporaneously with precipitation of authigenic

Table 2
Bulk rock XRD summary.

Depth (TVDgl)	Illite/Smectite (%)	Illite + Mica (%)	Kaolinite (%)	Chlorite (%)	Quartz (%)	K Feldspar (%)	Plagioclase (%)	Calcite (%)	Pyrite (%)
5161.19	1.63	2.62	2.44	1.64	61.63	8.21	21.82	TR	0
5162.38	1.73	3.37	2.13	2.16	63.00	7.89	19.72	TR	0
5162.88	1.05	2.59	4.35	2.14	60.93	9.81	19.14	0	0
5163.38	1.20	6.18	11.97	5.10	47.39	9.91	16.95	0	1.29
5164.17	1.51	2.62	4.25	1.93	62.69	7.78	18.33	0	0.88
5167.16	1.32	9.83	7.86	8.66	47.72	6.59	18.03	0	0.00
5167.56	1.48	3.07	1.17	2.76	65.09	6.86	18.57	1.00	0
5168.36	1.60	3.52	3.44	3.68	54.84	10.29	21.21	0	1.42
5168.76	1.20	9.98	5.00	5.14	49.92	9.17	19.59	0	0
5169.25	1.36	2.79	2.11	3.01	59.37	8.53	22.83	0	0
5492.78	1.63	3.05	2.13	3.80	61.46	6.40	20.16	1.37	0
5493.87	1.31	2.52	2.70	3.06	58.68	7.82	21.71	2.20	0
5494.96	1.23	6.26	1.64	2.51	59.00	6.60	19.06	3.70	0
5495.85	1.72	8.27	4.14	4.12	59.41	5.61	16.74	0	0
5496.65	TR	6.74	2.42	1.84	28.18	4.92	13.07	32.82	10.02
5496.75	1.56	9.01	3.21	2.96	53.22	6.61	21.03	2.40	0

Table 3
Clay Fraction (< 2 μm) XRD summary.

Depth	Wt. %	Illite/smectite				Illite			Kaolinite			Chlorite			Quartz		Calcite	
(TVDgl)	< 2 μm	% A	% B	Order	% Illite	% A	% B	Crys	% A	% B	Crys	% A	% B	Crys	% A	% B	% A	% B
5161.19	3.2	50.5	1.6	RI/O	50–60	7.9	0.2	P	29.5	0.9	M	10.3	0.3	P	1.8	0.1	0	0
5162.38	3.1	56.8	1.7	RI/O	50–60	8.4	0.3	P	19.2	0.6	M	12.2	0.4	P	3.5	0.1	0	0
5162.88	2.5	40.6	1.0	RI/O	50–60	9.4	0.2	P	36.0	0.9	M	11.6	0.3	P	2.4	0.1	0	0
5163.38	3.7	33.3	1.2	O	60–80	17.0	0.6	P	34.2	1.3	M	13.9	0.5	P	1.7	0.1	0	0
5164.17	3.0	48.1	1.5	RI/O	50–60	7.7	0.2	P	28.7	0.9	M	14.3	0.4	P	1.3	0.0	0	0
5167.16	4.4	28.6	1.3	O	60–80	23.2	1.0	P	22.6	1.0	M	23.1	1.0	P	2.6	0.1	0	0
5167.56	2.7	55.1	1.5	O	60–80	9.8	0.3	P	12.9	0.3	P	19.9	0.5	P	2.3	0.1	0	0
5168.36	3.1	50.7	1.6	O	60–80	11.1	0.3	P	17.4	0.5	P	18.9	0.6	P	2.0	0.1	0	0
5168.76	2.8	43.5	1.2	O	60–80	13.5	0.4	P	21.2	0.6	P	19.9	0.6	P	1.8	0.1	0	0
5169.25	2.5	55.6	1.4	O	60–80	14.0	0.4	P	12.1	0.3	P	15.4	0.4	P	3.0	0.1	0	0
5492.78	3.1	51.3	1.6	RI/O	50–60	11.4	0.4	P	13.0	0.4	P	21.0	0.7	P	3.2	0.1	0	0
5493.87	2.8	47.0	1.3	RI/O	50–60	16.1	0.5	P	18.2	0.5	P	16.8	0.5	P	2.0	0.1	0	0
5494.96	3.1	39.4	1.2	RI/O	50–60	16.5	0.5	P	20.2	0.6	P	21.6	0.7	P	2.3	0.1	0	0
5495.85	3.8	44.3	1.7	RI/O	50–60	11.7	0.4	P	23.5	0.9	P	18.0	0.7	P	2.6	0.1	0	0
5496.65	3.0	TR	TR	RI/O	50–60	0.0	0.0	P	59.3	1.8	P	29.7	0.9	P	1.1	0.0	9.9	0.3
5496.75	3.7	43.9	1.6	RI/O	50–60	11.6	0.4	P	23.3	0.9	P	19.7	0.7	P	1.5	0.1	0	0

A = Weight % relevant size fraction
B = Weight % bulk sample
Mixed-layer Ordering:
R I = Randomly Interstratified (R0)
O = Ordered Interstratification (R1)
Crystallinity:
M = Moderately Crystallised
P = Poorly Crystallised

chlorite, smectite and kaolinite, which is shown by clay mineral pore infilling and overgrowth of dissolution cavities in degraded feldspar grains (Fig. 9a). BSEM analysis displays pervasive filling of pores with kaolinite (Fig. 9c), and is dramatically increased where the highest feldspar degradation occurs (Table 3). Large kaolinite filled pores, which are often the same size as former detrital grains, indicates shallow, early diagenesis, leading to the formation of a grain framework.

Fluid inclusion data collected by Higgs et al. (2013) suggests that quartz cementation initiated at approximately 90 °C in the Kapuni Field, with the main phase occurring between 100 °C and 130 °C. The temperature history shows that the relatively minor amount of quartz cement in Farewell Formation formed from the Mid-Eocene to the present-day with most precipitation occurring during the last 20 My. This major phase will have occurred at depths below 3500 m, after significant porosity reduction by mechanical compaction.

Limited amounts of micro and macro-quartz were precipitated in the Farewell Formation and, sourced from sutured grains (Figs. 8a and 9c) and feldspar dissolution reactions. The current formation temperatures of > 130 °C and lack of grain coating clays provides the perfect environment for nucleation and growth of pervasive quartz cement, but only limited overgrowths have been identified. The general lack of quartz cementation at these elevated temperatures could be explained through the early destruction of porosity and permeability in sandstone beds, limiting the rate of diffusion of dissolved solutes and restricted space for the growth of macro-quartz. The feldspar degradation reactions and subsequent clay reactions will have liberated silica, which would have led to the observed limited quartz cementation.

The Illite:smectite ratio is as high as 60% in certain samples (Table 3). By burial heating to 120 °C it can be expected that the vast majority of smectite would have transformed into Illite. The high K-feldspar content (Table 2) of the bulk rock excludes potassium availability as a limiting factor, but the exceptionally low porosity and permeability could have restricted flow and caused slow diffusion, further inhibited by hydrocarbon charging. The majority of the Illite/smectite is randomly interstratified with only a few ordered interstratified occurrences, which infers that the process is on-going (Table 3).

The occurrence of Kaolinite in secondary dissolution pore space often displays an undercompacted form and associated micro porosity can be filled with hydrocarbons during the later stage of burial. A similar form of kaolinite has also been identified in the Mangahewa Formation at Cardiff-1 (Higgs et al., 2007). Additional evidence for continued feldspar dissolution and kaolinite precipitation comes from the pattern of oil staining observed in some kaolinite in thin-sections. Both stained and unstained kaolin are observed within a single thin-section, a feature identified in deep arkosic sediments in the central North Sea where variable staining is indicative of growth after charging, on-going dissolution, and low reservoir quality (Wilkinson et al.,

Table 5
Petroleum inclusion fluorescence summary.

Depth (mMDAH)	n	Flourence Colour	Av. API
5185.7	39	blue-green	29.3
5189.1	3	blue-green	33.1
5516.1	8	blue-green	35.2
5518.1	28	blue-green	25.9
5519.0	5	blue-green	32.7

Table 4
Fluid inclusion microthermometry summary.

Depth (mMDAH)	5183.7		5518.1	
Host	Detrital quartz grain, fracture fill	Detrital quartz grain, fracture fill	Detrital quartz grain, fracture fill	Detrital quartz grain, fracture fill
Type	secondary, oil assoc	secondary	secondary, oil assoc	secondary
Contents	aqueous	oil	aqueous	oil
Average Hom Temp (°C)	113.4	70.7	116.6	68.6
Min Hom Temp (°C)	106.1	69.0	114.1	41.2
Max Hom Temp (°C)	121.7	73.3	119.6	76.0
n	5.0	7.0	3.0	16.0
Standard Deviation	6.0	1.4	2.8	10.6

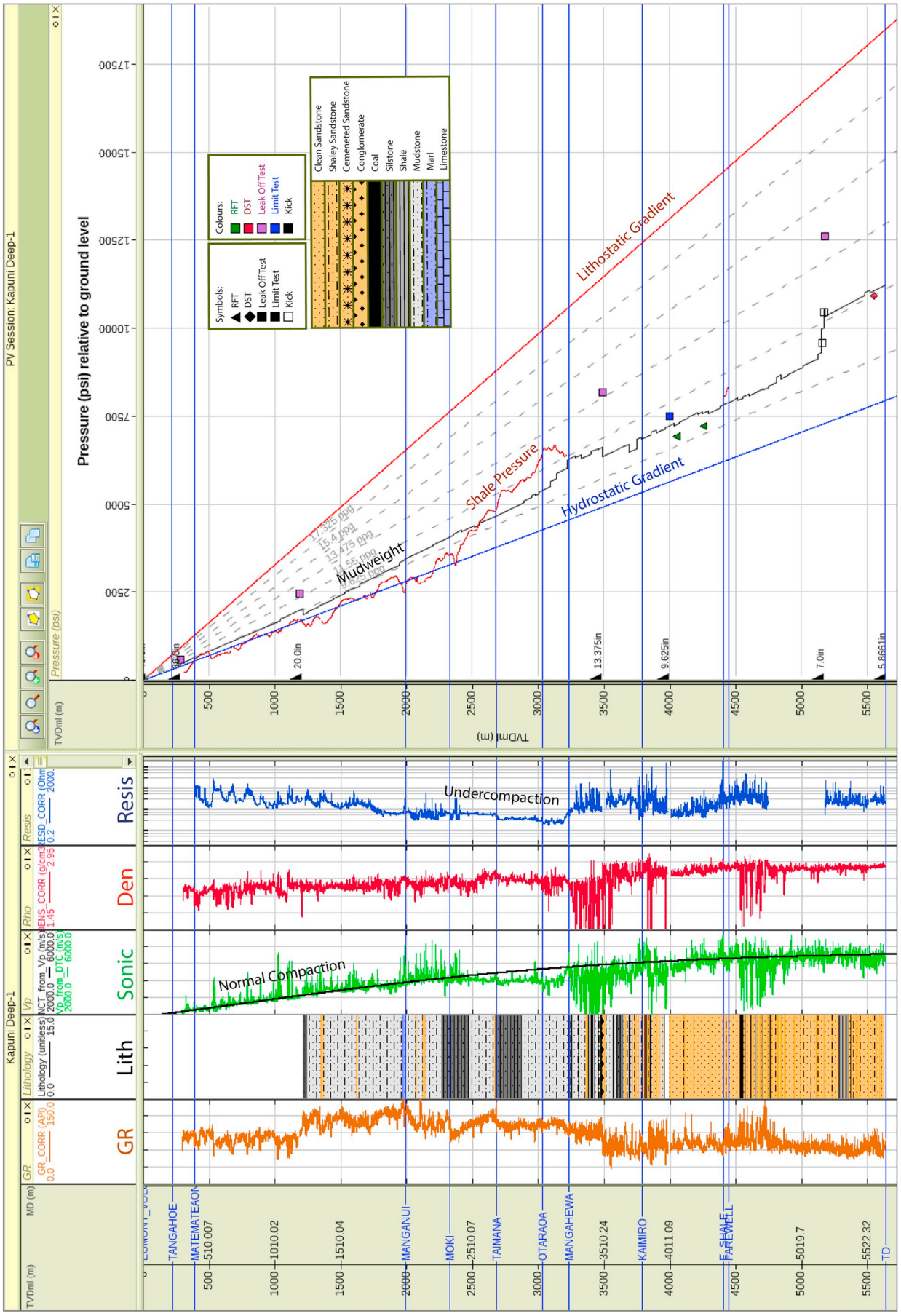

Fig. 10. a) 1D burial history plot of Kapuni Deep-1 (Petromod). Red lines are isotherms and colour overlay denotes pore pressure. Blue rectangle-aqueous fluid inclusions within quartz filled fractures, where microthermometry suggests trapping temperatures of 105–125 °C (av. 110 °C); b) Plot displaying the evolution of overpressure and effective stress with burial since the deposition of the farewell Formation. (For interpretation of the references to colour in this figure legend, the reader is referred to the Web version of this article.)

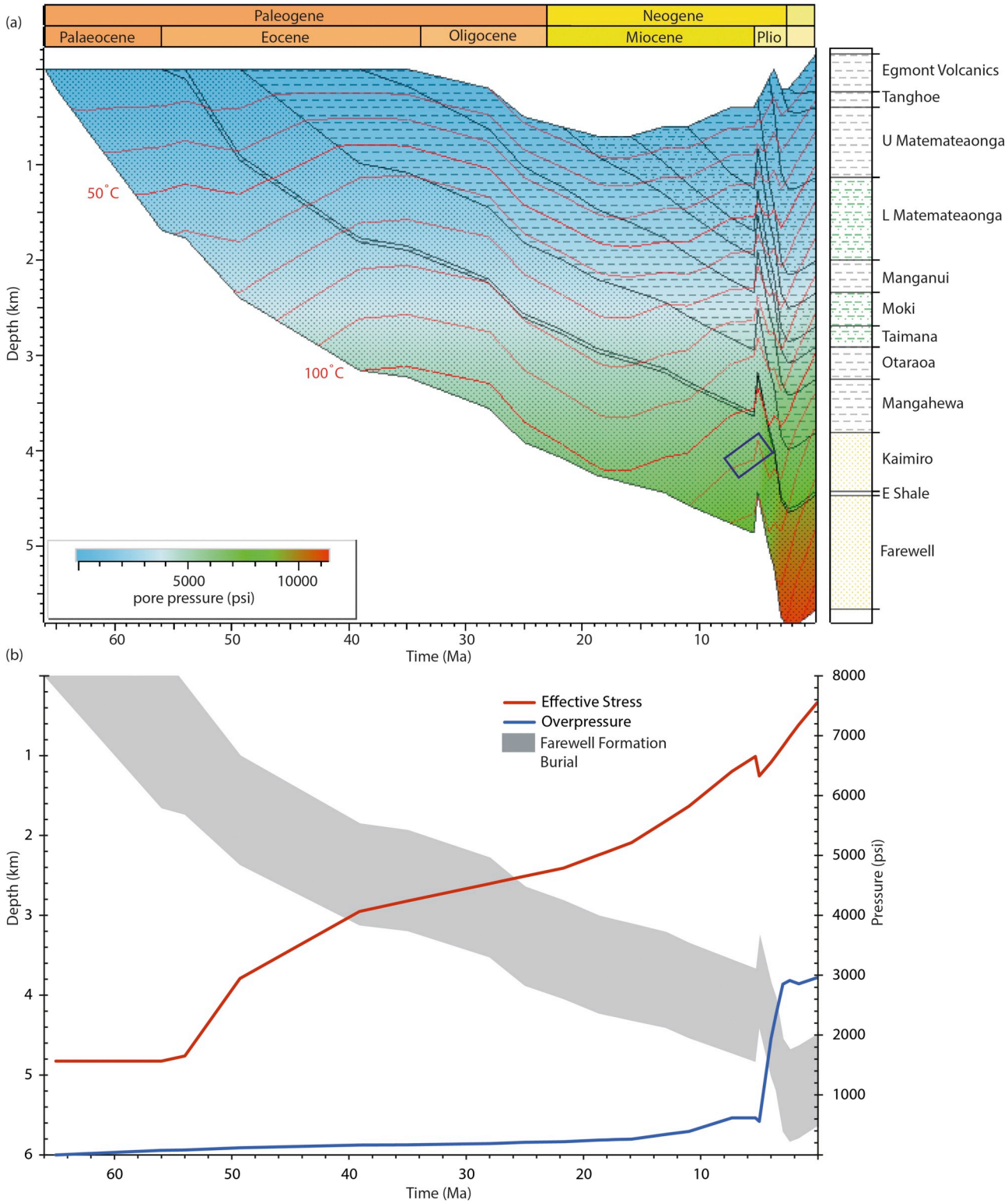

Fig. 11. Kapuni Deep-1 pressure depth plot with the suite of wireline measurements (Gamma Ray, sonic (interval transit time [ITT]), resistivity, and density, a summary lithologic column, normal compaction trend [NCT], RFT pressure measurements [green triangles], Drill stem tests [red triangle], kicks [white square], leak-off pressure [purple squares], limit tests [blue squares], mud-weight profile [black], shale pressure [red]). (For interpretation of the references to colour in this figure legend, the reader is referred to the Web version of this article.)

2014).

Kaolinite becomes unstable with increasing formation temperature and is rarely preserved above 100 °C (Bjørkum and Gjelsvik, 1988), suggesting that there is an anomalously high content based on measured formation temperatures for the Farewell Formation in this study. The supply of potassium is commonly ascribed as a limiting factor in the conversion of kaolinite to illite and usually sourced from k-feldspar dissolution (e.g. Bjørkum and Gjelsvik, 1988). The abundance of kaolinite in the Farewell formation reservoirs of the Kapuni deep-1 well is attributed to effect of recent and rapid burial with insufficient time at

current formation temperatures for diagenetic reactions to have equilibrated and allow illitization of kaolinite.

The low abundance of hydrocarbon inclusions within the already rare quartz overgrowths in both of the Kapuni Deep-1 cores suggests that the reservoir quality was very poor during charging. Most clays are poorly crystalline with only a small number of kaolinite samples being moderately crystalline, which indicates very little space for growth. The low abundance and anhedral nature of quartz overgrowths, coupled with the lack of fluid inclusions and poorly crystalline clays, supports evidence for low porosity and permeability.

The aqueous inclusions measured from quartz-filled fractures give an average homogenisation temperature of 110 °C (Table 4), which when compared with the burial history will have been trapped between 6 and 4 Ma. Higgs et al. (2013) suggested that Palaeogene coals matured for oil during the past 2 M y. and are therefore are a likely source for oil in the Farewell Formation. This is supported by a range in API gravities that indicate moderate maturities, which is indicative of late generation and charging. The presence of bitumen in fractures (Fig. 13) suggests that they formed in the past 2 M y. associated with the expulsion of oil from interbedded coals (Higgs et al., 2013), which was subsequently thermally cracked due to increasing temperatures during rapid Pliocene burial (Kukla et al., 2011; Schoenherr et al., 2007).

The present-day reservoir quality of the Farewell Formation is a cumulative product of depositional attributes, mechanical compaction and diagenesis during early and later stages of burial (Fig. 12). Compaction and the growth of authigenic clay and carbonate cement are the most significant diagenetic processes occurring in the Farewell Formation at Kapuni Deep-1. The COPL-CEPL analyses, grain fracturing, very low helium porosities and IGVs shows that mechanical compaction was the key driving mechanism for porosity reduction during the first 3500 m of burial through the steady increase of vertical effect stress, which has been demonstrated by basin modelling (Fig. 7f).

4. Discussion

Measured porosity in the Farewell Formation at Kapuni Deep-1 are anomalously low for the current depth of burial and require explanation. Such low porosity is consistent with high vertical effective stress, partly explained by vertically and laterally expelled fluids prior to c.6 Ma such that no overpressure was maintained. Only after this period was overpressure retained.

4.1. Overpressure maintenance

The Farewell Formation has been allowed to dewater during continued burial, via vertical fluid escape and lateral drainage through high permeability pathways in the Cretaceous and Palaeocene (Fig. 14), which has inhibited the generation of overpressure. Lateral drainage has been identified across the Kupe South Field, where reservoir overpressures are less than intra-reservoir shales, caused by fluid pressure loss through interbedded sands of Cretaceous Puponga Member (Webster et al., 2011). This signature has also been identified in the Kapuni Field. Fig. 14 displays the decrease in reservoir overpressure in the Palaeocene towards the south from Kapuni Deep-1 through to Momoho-1. The Cretaceous and Palaeocene represent a continuous connected pathway for pressure dissipation until they outcrop on the sea floor and on the South Island (Figs. 1 and 14). Since c.6 Ma the Farewell Formation has been able to maintain excess pressure, which has been generated through rapid Pliocene burial.

The exceptionally low permeability of the Farwell Formation will slow the transfer of pressure up dip, which would place the reservoir pressure in closer equilibrium with the shale pressure and explain the continued maintenance. The lateral drainage of pressure would also be inhibited through the compartmentalisation. The current Kapuni Field seismic reflection data is of very poor quality, but dipmeter data, albeit only acquired over short intervals, indicates some structural disturbance between 4612 and 5287 mTVDgl, and it is possible that there is a significant sealing fault cutting the section in the data gap at c. 5160 m TVDgl. The presence of sealing faults in the region is supported by comparison of virgin pore pressures from Cardiff-1 and the Kapuni Field. The K3E reservoir pressure at Cardiff-1 is significantly higher there than in Kapuni Field (Webster et al., 2011), so there must be a lateral hydraulic barrier between them or the system is not in equilibrium. However, this structural configuration would still require a top seal to be effective.

4.2. Vertical effective stress and reservoir quality

Paxton et al. (2002) suggest that for overpressure/low VES to arrest mechanical compaction in reservoirs, abnormal pressures must develop at depths shallower than 2500 m, or within the depth window that mechanical compaction is active. As previously discussed the onset of overpressure occurred below 3500 mTVDgl in Farewell Formation during 6–2 Ma. after significant mechanical compaction.

The Magnolia Field, Gulf of Mexico (Sathar and Jones, 2016) and the Kessog Structure in the North Sea (Grant et al., 2014) are at equivalent depths, and display very similar immature reservoir composition to the Farewell Formation, but have markedly lower VES and excellent reservoir quality. Magnolia reservoirs have a vertical effective stress range between 5 and 25 MPa, and Kessog has 14 MPa, whereas the Farewell Formation at Kapuni Deep-1 has 45 MPa (lithostatic gradient 1 psi/ft [22.62 MPa/km]). The deep and late onset of abnormal pressure only allowed the formation of limited amounts of overpressure, which is not at a significant enough magnitude to arrest any further mechanical compaction and occurred after the Farewell Formation sandstones entered the chemical compaction window.

4.3. Intergranular volume

Mechanical compaction is characterised by the reorientation and repacking of competent (brittle) grains by local fracture or cleavage of brittle grains, and by plastic deformation of ductile grains (Houseknecht, 1987). Mechanical compaction alone has the potential to reduce intergranular volume to a minimum of 26%, assuming moderately to well sorted, well rounded and fairly spherical grains (Paxton et al., 2002). The overlying Mangahewa Formation at Cardiff-1 (Fig. 1) displays IGVs of av. 15%, but this further reduction has been attributed to chemical compaction (Higgs et al., 2007).

Intergranular volumes of between 6 and 11% in the Farewell Formation at Kapuni Deep-1 are significantly lower than 26%. The presence of detrital mud clasts, mica and lithic fragments would reduce the initial porosity of the sandstone beds. These ductile grains combined with the poorly sorted nature of the sandstone beds allows for grain reorientation and sliding resulting in more efficient packing, and plastic deformation during burial further reduces the IGV (Worden et al., 2000).

The relatively deep onset and restricted nature of quartz cementation in Farewell Formation, would allow mechanical compaction to continue at high stress further reducing the intergranular volume (Chuhan et al., 2002). Although grain crushing is not common in very fine to fine grained sandstones, the poorly sorted angular nature of the grains led to increased stress at sharp contacts, increasing the potential for grain fracturing and a reduction in intergranular volume. This is supported by the presence of healed fractures observed in false colour cathodoluminescence images (Fig. 9f).

Basin modelling carried out on the Kapuni Field by (Higgs et al., 2013) suggests that thermal maturation of thick organic rich coaly source rocks within Farewell and Rapoki Formations (Fig. 2) led to the generation and expulsion of large volumes of acidic fluids from c.60 Ma, thus enabling the dissolution of grain rims during shallow burial, weakening the grain framework and aiding in mechanical compaction. The onset of chemical compaction greatly reduces mechanical

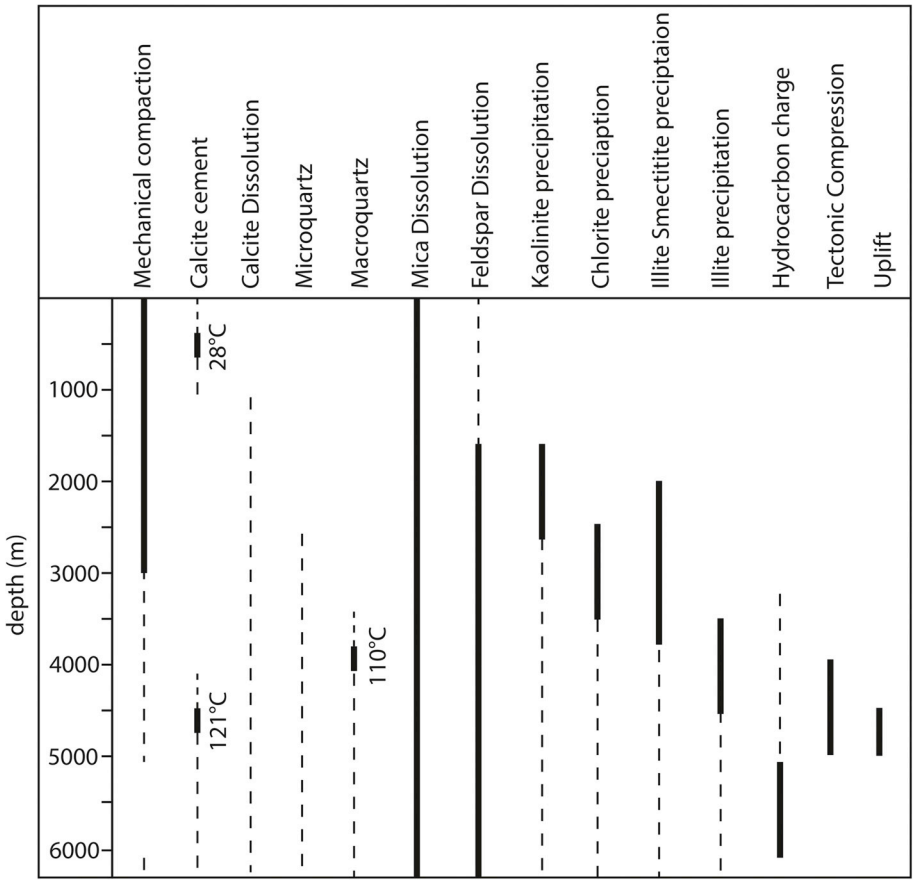

Fig. 12. Diagenetic Paragenesis for Farewell Formation sandstone beds in Kapuni Deep-1.

compaction (Chuhan et al., 2003), but the continued flushing of CO_2 rich fluids will be on-going, stimulating grain rim dissolution, which will reduce the strength of the grain framework and lead to further mechanical compaction.

4.4. CO_2 and secondary porosity

The flow of acidic rich fluids will have been an important mechanism in driving dissolution of carbonate cements and the generation of secondary porosity in the Kapuni Field (Higgs et al., 2013), producing oversized pores in some Taranaki reservoirs (Collen and Newman, 1991). Local patches of etched carbonate cement have been identified (Collen, 1988) along bitumen-filled fractures (Fig. 13) and in the upper core, as observed in Fig. 8b, implying that more extensive patches may have existed. The dissolved CO_2 in the pore fluids will also have driven feldspar dissolution, producing secondary porosity, but also have provided ions for precipitation of authigenic clays and quartz cements filling pore space elsewhere. This would lead to further compartmentalisation by formation diagenetic barriers to flow and aid in the maintenance of abnormal pressure.

4.5. Deep pressure transition

The origin of the pressure transition zone within the Farewell

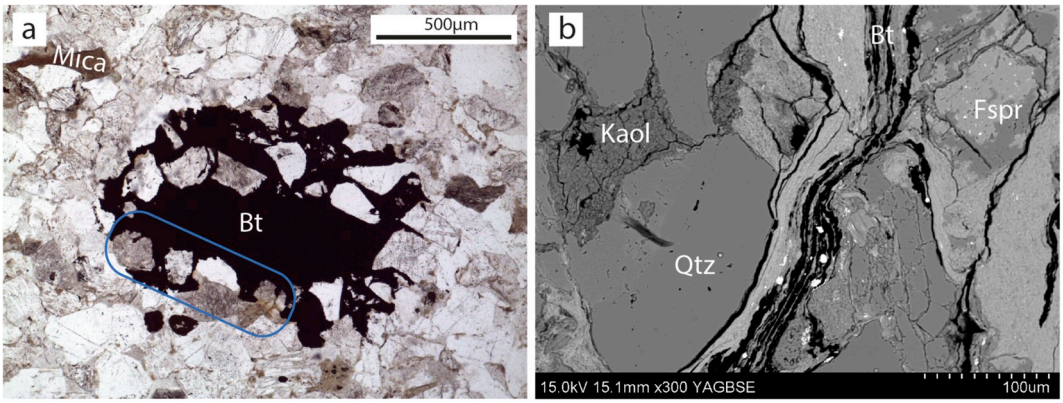

Fig. 13. a) Thin section micrograph (5183.7 mMDAH): cross section through a fracture filled with bitumen displaying edged grains around the rim (blue rectangle); (b) BSEM image (5518.1 mMDAH): bitumen filled fractures, clay smear and pore filling kaolinite (Bt = bitumen; Kaol = kaolinite; Qtz = quartz; Fspr = feldspar). (For interpretation of the references to colour in this figure legend, the reader is referred to the Web version of this article.)

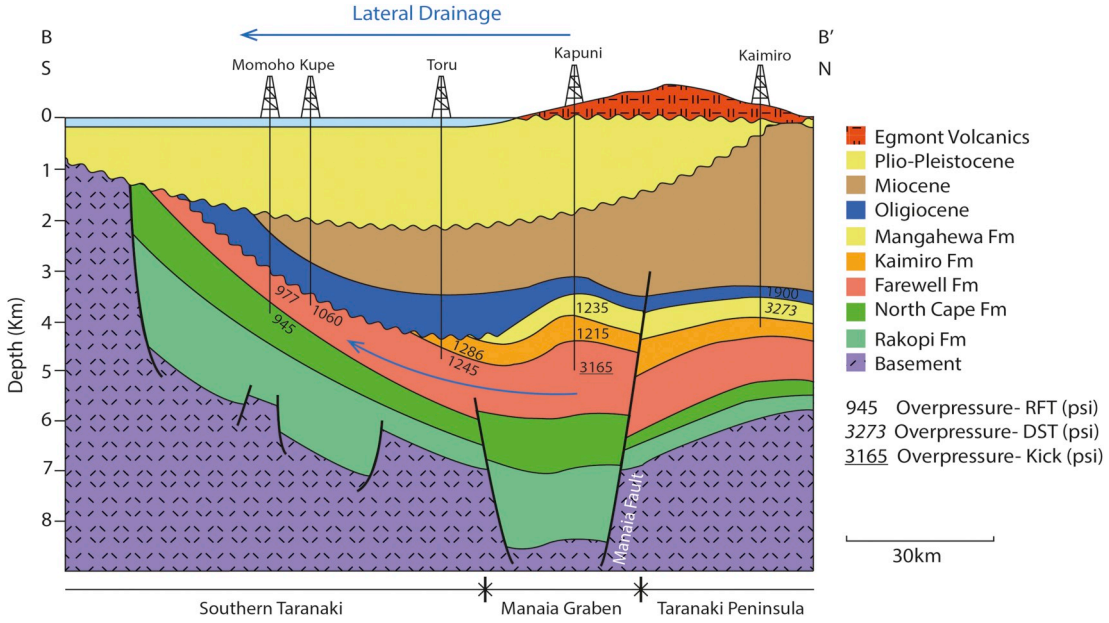

Fig. 14. Cross section (line B-B′, Fig. 1) displays lateral drainage in the Southern Taranaki (Modified from (King and Thrasher, 1996).

Formation is not clear, as there is no obvious change in the wireline signature, indicating a subtle change in reservoir properties below the resolution and sensitivity of the wireline tools.

Webster et al. (2011) suggested kerogen cracking as a secondary overpressure mechanism, which could account for increased pressure below 5000 m. Swarbrick et al. (2002) show that kerogen transformation/gas generation has the potential to produce overpressures of 70–6000 psi/0.5–41 MPa, at equivalent maturity expected in the Cretaceous of Taranaki Basin. Kukla et al. (2011) showed that a self-charging interbedded source rock reservoir system, similar to the Farewell Formation, contributed 435 psi/3 MPa of overpressure to a Neoproterozoic system in Oman. However the Farewell Formation was only mature for oil during the past 2 Ma, but the low reservoir permeability would inhibit the contribution to the overpressure.

Furthermore the transition could be attributed to an effective vertical pressure seal, as even thin shale intervals can support a significant pressure differential, demonstrated by a 1595 psi (11 MPa) increase in pore pressure in less than 50 m in two fields of the Baram Delta (Tingay et al., 2009). Wireline signatures suggest that Palaeogene shales in Farewell Formation are poorly developed to act as effective seals. However one potential unit, the 135 m-thick E shale (Fig. 6a), is a transgressive interval found at the base of the Kaimiro Formation, comprised of sandy, light to moderate grey calcareous siltstone, which passes up into dark brown calcareous shale (STOS, 1984). Increases in density and velocity and reduction in gamma ray of the E shale are all indicative of a fine grain size lithology.

4.5.1. Secondary compaction

The Farewell Formation pressure transition zone occurs in a thick sandstone package, which under normal circumstances would not act as a pressure seal., However, Weedman et al. (1992) proposed a model whereby early cementation allows loosely packed sandstones to subside to significant depths (equivalent to the Farewell Formation at Kapuni Deep-1) followed by dissolution of these early carbonate cements. The ensuing compaction of sandstones creates zones of extremely low permeability, which act with interbedded shales to form a pressure seal (Weedman et al., 1992).

The study of Weedman et al. (1992) was undertaken in the Upper Cretaceous Tuscaloosa Formation of onshore Louisiana, USA, which displays similar reservoir characteristics of interbedded sandstone and shales and sandstone connectivity to the Farewell Formation. There are multiple sources of pressure generation attributed to deep basin overpressure (e.g. Osborne and Swarbrick, 1997; Swarbrick et al., 2002), but an effective barrier to vertical migration out of the Farewell Formation is needed to explain the present overpressure transition (1900 psi/13 MPa) between the measured pressures in the Kaimiro and Farewell Formations (Fig. 10). In the absence of a laterally extensive thick mudrock to act as a vertical sealing mechanism, it is proposed that migration of acidic CO_2-rich pore fluids, already identified as an important dissolution process in the Kapuni Field (Higgs et al., 2013), could have created a pressure transition zone. Precipitation of early carbonate cements have been recognised in the Farewell Formation and are likely sites for secondary porosity generation through dissolution with subsequent extreme secondary compaction and corresponding permeability reduction (e.g. Weedman et al., 1996, 1992).

4.6. Implications for deeply buried sandstone reservoirs

Reservoir sandstones with high porosity (10%–30%) and overpressures are encountered at > 2 km depths in many sedimentary basins (Weedman et al., 1992). This investigation has demonstrated that this is not always the case, being dependent on the stress history and stratigraphic stacking of the basin fill. The Farewell Formation has experienced a continued increase in VES during burial which drove porosity loss through mechanical compaction. Consequently the late and deep onset of abnormal pressures at Kapuni Deep-1 has meant that the pore pressure regime is, in part, controlled by the diagenetic evolution of the reservoirs.

However, burial histories of tectonically disparate parts of the Taranaki Basin, primarily its northern parts, display early rapid and continued burial of thick packages of marine mudstone inter-fingered with high quality deep-water sandstone deposits. This stratigraphic configuration and burial history is ideal for the generation and maintenance of low vertical effective stress conditions, which could arrest porosity loss in associated inter-fingering sandstone beds.

Early pore filling and late precipitation of calcite cement in partially or fully dissolved quartz and feldspars grains has produced secondary intergranular volumes of up to 42%, which has the potential to produce substantial secondary porosity. Higgs et al. (2013) suggested that in Kaimiro and Mangahewa Formations, which overlie Farewell Formation, these CO_2 rich fluids preferentially flow through vertically stacked, coarse sandstone facies, resulting in the generation of

significant secondary porosity. Less feldspar reaction occurred in fine sandstone from heterolithic intervals, yet overall, more secondary minerals have precipitated. This implies that there has been a net redistribution of ions from coarse cleaner beds to fine heterolithic beds, and that this diagenetic redistribution has led to enhanced vertical reservoir heterogeneity (Higgs et al., 2013). The cored sections of Farewell Formation sandstone at Kapuni Deep-1 are very fine to fine with poor sorting and abundant labile grains and detrital clay. Ions from reactions could have migrated in pore fluids from coarser units and then precipitated as secondary minerals within the low permeability beds, further reducing reservoir quality. Conversely, it could be expected that coarser units of enhanced reservoir quality could exist at depth in the Farewell Formation, producing alternating cemented zones and enhanced porosity intervals.

The zones of focused fluid flow and potentially increased porosity and permeability could act as 'valves' that are at risk from local collapse during secondary compaction, producing diagenetic pressure barriers as postulated for the Farewell Formation pressure transition zone. By analogy with observations from the Moore-Sams Field, Tuscaloosa Trend, USA reported by Weedman et al. (1992) the Farewell Formation may have developed internal pressure barriers, which could have led to the current distribution of overpressure beneath a pressure transition zone. The mechanism for the fluid barrier is "secondary" compaction caused by dissolution of cements. The sporadic nature and sometimes very pervasive carbonate cement, makes it very difficult to predict where these low permeability secondary compacted zones could occur.

Mapping out and predicting the diagenetic paragenesis of deep sandstone reservoirs poses many issues, which are further complicated by the flow of aggressive reactive pore fluids. Furthermore, common bitumen-filled fractures (Fig. 13) along with natural fractures identified in reservoirs deeper than 4000 m elsewhere in the Taranaki Basin (Webster et al., 2011) hold the potential to further enhance permeability or conversely increase compartmentalisation (Schoenherr et al., 2007).

5. Conclusions

1) Mechanical compaction driven by initial rapid subsidence has been the key mechanism for porosity reduction in the Farewell Formation during the first 3000 m of burial. The low IGV, concavo-convex and quartz-to-quartz long grain contacts, anhedral nature of quartz overgrowths, general lack of fluid inclusions, and poor crystalline clay mineral content indicate that reservoir quality was markedly reduced by early burial compaction processes.
2) The absence of significant intervals of low permeability fine-grained strata within Palaeocene and Eocene section has allowed the reservoirs to dewater during burial inhibiting the preservation of any overpressures, documenting a history involving high vertical effective stress. .
3) High sedimentation rates and associated rapid burial in the Pliocene generated late overpressure through disequilibrium compaction in the Oligocene to early Miocene sections during this period, but had little or no impact on reservoir quality of the Farewell Formation. The retention of the late overpressure is attributed to the severe reduction of permeability during cement dissolution and secondary compaction.
4) Late and rapid burial has not allowed sufficient time for clay mineral transformation to take place, with Farewell Formation displaying anomalously high kaolinite content and high Illite:smectite ratios relative to the present day formation temperatures.
5) Continued compaction of Farewell Formation sandstones after dissolution of early carbonate cements creates zones of extremely low permeability, which has the potential to act with interbedded shales to form a pressure seal as seen in the deep section of the Kapuni Field.
6) Depositional facies and early diagenetic cements within the Farewell Formation play an important role in defining the pore pressure and must be included when predicting the geopressure regime in the deeper sections of the Taranaki Basin.
7) The resolution of a diagenetic paragenesis for the Farewell Formation has important implications for hydrocarbon exploration and prospect development in deep parts (> 4500 mTVD) of the underexplored areas in Taranaki Basin.

Acknowledgements

The work contained in this paper was conducted during a PhD study undertaken as part of the Natural Environment Research Council Centre for Doctoral Training (CDT) in Oil & Gas [grant number NEM00578X/1] and is fully funded by NERC whose support is gratefully acknowledged. The authors would also like to thank Rob Funnell (GNS) for bottom hole temperature data for the Kapuni Field; J.M. Utley for QEMSCAN analyses; Leon Bowen for advice on SEM analyses and IKON Science and Schlumberger for the use of RokDoc and PetroMod software. The manuscript was improved after discussions with Stephan Stricker, Andy Aplin and Robert Crookbain. The authors thank Peter Kukla and one anonymous reviewer for their constructive comments.

References

Armstrong, P.A., Allis, R.G., Funnell, R.H., Chapman, D.S., 1998. Late Neogene exhumation patterns in Taranaki Basin (New Zealand): evidence from offset porosity-depth trends. J. Geophys. Res. Earth 103, 30269–30282. https://doi.org/10.1029/98JB02843.

Armstrong, P.A., Chapman, D.S., 1999. Combining tectonics and thermal fields in Taranaki basin, New Zealand. In: Förster, A., Merriam, D.F. (Eds.), Geothermics in Basin Analysis. Springer US, Boston, MA, pp. 151–176. https://doi.org/10.1007/978-1-4615-4751-8_8.

Atkinson, J.H., Bransby, P.L., 1978. The Mechanics of Soils: an Introduction to Critical State Soil Mechanics. McGraw-Hill.

Bjørkum, P.A., Gjelsvik, N., 1988. An isochemical model for formation of authigenic kaolinite, K-Feldspar and illite in sediments. J. Sediment. Petrol. 58, 506–511.

Burgreen-Chan, B., Meisling, K.E., Graham, S., 2016. Basin and petroleum system modelling of the East Coast Basin, New Zealand: a test of overpressure scenarios in a convergent margin. Basin Res. 28, 536–567. https://doi.org/10.1111/bre.12121.

Burn, M., Crookbain, R., Bourke, A., 1995. Kapuni Group Core Description and Digital Logging, Onshore Taranaki Basin. Unpublished Petrocorp Report Number 0684.

Chuhan, F.A., Kjeldstad, A., Bjørlykke, K., Høeg, K., 2003. Experimental compression of loose sands : relevance to porosity reduction during burial in sedimentary basins. Can. Geotech. J. 1011, 995–1011. https://doi.org/10.1139/T03-050.

Chuhan, F.A., Kjeldstad, A., Bjùrlykke, K., Hùeg, K., 2002. Porosity loss in sand by grain crushing - experimental evidence and relevance to reservoir quality. Mar. Petrol. Geol. 19, 39–53. https://doi.org/10.1016/S0264-8172(01)00049-6.

Collen, J.D., 1988. Diagenetic control of porosity and permeability in Pakawau and Kapuni group sandstones, Taranaki basin, New Zealand. Energy Explor. Exploit. 6, 263–280. https://doi.org/10.1177/014459878800600307.

Collen, J.D., Newman, R.H., 1991. Porosity development in deep sandstones, Taranaki Basin, New Zealand. J. Southeast Asian Earth Sci. 5, 449–452. https://doi.org/10.1016/0743-9547(91)90060-B.

Crowhurst, P.V., Green, P.F., Kamp, P.J.J., 2002. Appraisal of (U-Th)/He apatite thermochronology as a thermal history tool for hydrocarbon exploration: an example from the Taranaki Basin, New Zealand. Am. Assoc. Petrol. Geol. Bull. 86, 1801–1819. https://doi.org/10.1306/61EEDD82-173E-11D7-8645000102C1865D.

Darby, D., 2002. Seal properties , overpressure and stress in the taranaki and East Coast basins , New Zealand. In: 2002 New Zealand Petroleum Conference Proceedings, pp. 1–10.

Franks, S.G., Forester, R.W., 1984. Relationships among secondary porosity , pore-fluid chemistry and carbon dioxide , Texas Gulf coast. In: Mcdonald, D.A., Surdam, R.C. (Eds.), Clastic Diagenesis. American Association of Petroleum Geologists, pp. 63–79.

Funnell, R., Chapman, D., Allis, R., Armstrong, P., 1996. Thermal state of the Taranaki basin, New Zealand. J. Geophys. Res. 101, 25197. https://doi.org/10.1029/96JB01341.

Grant, N.T., Middleton, A.J., Archer, S., 2014. Porosity trends in the Skagerrak formation , central Graben , United Kingdom continental Shelf : the role of compaction and pore pressure history. Am. Assoc. Petrol. Geol. Bull. 6, 1111–1143. https://doi.org/10.1306/10211313002.

Hantschel, T., Kauerauf, A.I., 2009. Fundamentals of basin and Petroleum Systems Modeling, Fundamentals of Basin and Petroleum Systems Modeling. Springer-Verlag, Berlin. https://doi.org/10.1007/978-3-540-72318-9.

Higgs, K.E., Funnell, R.H., Reyes, A.G., 2013. Changes in reservoir heterogeneity and quality as a response to high partial pressures of CO_2 in a gas reservoir, New Zealand. Mar. Petrol. Geol. 48, 293–322. https://doi.org/10.1016/j.marpetgeo.2013.08.005.

Higgs, K.E., Strogen, D.P., Griffin, A., Ilg, B.R., Arnot, M.J., 2012. Reservoirs of the Taranaki Basin, New Zealand. GNS Science Data Series No. 2012/13a.

Higgs, K.E., Zwingmann, H., Reyes, A.G., Funnell, R.H., 2007. Diagenesis, porosity evolution, and petroleum emplacement in tight gas reservoirs, Taranaki Basin, New Zealand. J. Sediment. Res. 77, 1003–1025. https://doi.org/10.2110/jsr.2007.095.
Hottmann, C.E., Johnson, R.K., 1965. Estimation of formation pressures from log-derived shale properties. J. Petrol. Technol. 17, 717–722. https://doi.org/10.2118/1110-PA.
Houseknecht, D.W., 1987. Assessing the relative importance of compaction processes and cementation to reduction of porosity in sandstones. Am. Assoc. Petrol. Geol. Bull. 71, 633–642.
Kamp, P.J.J., Green, P.F., 1990. Thermal and tectonic history of selected Taranaki Basin (New Zealand) wells assessed by apatite fission track analysis. Am. Assoc. Petrol. Geol. Bull. https://doi.org/10.1306/0C9B24E3-1710-11D7-8645000102C1865D.
Kamp, P.J.J., Tripathi, A.R.P., Nelson, C.S., 2014. Paleogeography of late Eocene to earliest Miocene Te Kuiti group, central-western North Island, New Zealand. New Zeal. J. Geol. Geophys. 57, 128–148. https://doi.org/10.1080/00288306.2014.904384.
Kamp, P.J.J., Vonk, A.J., Bland, K.J., Hansen, R.J., Hendy, A.J.W., McIntyre, A.P., Ngatai, M., Cartwright, S.J., Hayton, S., Nelson, C.S., 2004. Neogene stratigraphic architecture and tectonic evolution of wanganui, king country, and eastern taranaki basins, New Zealand. New Zeal. J. Geol. Geophys. 47, 625–644. https://doi.org/10.1080/00288306.2004.9515080.
Killops, S.D., Funnell, R.H., Suggate, R.P., Sykes, R., Peters, K.E., Walters, C., Woolhouse, A.D., Weston, R.J., Boudou, J.-P., 1998. Predicting generation and expulsion of paraffinic oil from vitrinite-rich coals. Org. Geochem. 29, 1–21. https://doi.org/10.1016/S0146-6380(98)00087-4.
King, P.R., Thrasher, G.P., 1996. Cretaceous-cenozoic Geology and Petroleum Systems of the Taranaki Basin, New Zealand. Institute of Geological and Nuclear Sciences, New Zealand Monograph 13, Ministry of Economic Development Petroleum Report 3224.
Kukla, P.A., Reuning, L., Becker, S., Urai, J.L., Schoenherr, J., 2011. Distribution and mechanisms of overpressure generation and deflation in the late Neoproterozoic to early Cambrian South Oman Salt Basin. Geofluids 11, 349–361. https://doi.org/10.1111/j.1468-8123.2011.00340.x.
Lahann, R.W., Swarbrick, R.E., 2011. Overpressure generation by load transfer following shale framework weakening due to smectite diagenesis. Geofluids 11, 362–375. https://doi.org/10.1111/j.1468-8123.2011.00350.x.
Lundegard, P.D., 1992. Sandstone porosity loss–a "big picture" view of the importance of compaction. J. Sediment. Petrol. 62, 250–260.
Martin, K.R., Baker, J.C., Hamilton, P.J., Thrasher, G.P., 1994. Diagenesis and reservoir quality of Palaeocene sandstones in the Kupe South field, Taranaki basin, New Zealand. Am. Assoc. Petrol. Geol. Bull. 78, 624–643.
Mitchell, J.S., Mackay, K.A., Neil, H.L., Mackay, E.J., Pallentin, A., Notman, P., 2012. Undersea New Zealand, 1:5,000,000. NIWA Chart Miscellaneous Series No. 92.
Nelson, C.S., Kamp, P.J.J., Young, H.R., 1994. Sedimentology and petrography of mass-emplaced limestone (Orahiri Limestone) on a late Oligocene shelf, western North Island, and tectonic implications for eastern margin development of Taranaki Basin. New Zeal. J. Geol. Geophys. 37, 269–285. https://doi.org/10.1080/00288306.1994.9514621.
Nguyen, B.T.T., Jones, S.J., Goulty, N.R., Middleton, A.J., Grant, N., Ferguson, A., Bowen, L., 2013. The role of fluid pressure and diagenetic cements for porosity preservation in Triassic fluvial reservoirs of the Central Graben, North Sea. Am. Assoc. Petrol. Geol. Bull. 97, 1273–1302. https://doi.org/10.130e/01151311163.
O'Connor, S. a., Swarbrick, R.E., 2008. Pressure regression, fluid drainage and a hydrodynamically controlled fluid contact in the north sea, lower cretaceous, Britannia sandstone formation. Petrol. Geosci. 14, 115–126. https://doi.org/10.1144/1354-079308-737.
Osborne, M.J., Swarbrick, R.E., 1997. Mechanisms for generating overpressure in sedimentary basins: a reevaluation. Am. Assoc. Petrol. Geol. Bull. 81, 1023–1041. https://doi.org/10.1306/E4FD2D89-1732-11D7-8645000102C1865D.
Paxton, S., Szabo, J., Ajdukiewicz, J., Klimentidis, R., 2002. Construction of an intergranular volume compaction curve for evaluating and predicting compaction and porosity loss in rigid-grain sandstone reservoirs. Am. Assoc. Petrol. Geol. Bull. 86, 2047–2067.
Pryor, W.A., 1973. Permeability-porosity patterns and variations in some Holocene sand bodies. Am. Assoc. Petrol. Geol. Bull. 57, 162–189. https://doi.org/10.1306/819A4252-16C5-11D7-8645000102C1865D.
Rajabi, M., Ziegler, M., Tingay, M., Heidbach, O., Reynolds, S., 2016. Contemporary tectonic stress pattern of the Tarnaki Basin, New Zealand. J. Geophys. Res. Earth 121, 6053–6070. https://doi.org/10.1002/2016JB013178.Received.
Rattenbury, M.S., Cooper, R.A., Johnston, M.R., 1998. Geology of the Nelson Area. Institute of Geological & Nuclear Sciences Limited 1:250,000 Geological Map 0. Institute of Geological & Nuclear Sciences Limited, Lower Hutt, New Zealand.
Sathar, S., Jones, S., 2016. Fluid overpressure as a control on sandstone reservoir quality in a mechanical compaction dominated setting : Magnolia Field , Gulf of Mexico. Terra. Nova 28, 155–162. https://doi.org/10.1111/ter.12203.
Schmidt, D.S., Robinson, P.H., 1989. The structural setting and depositional history for the Kupe South field, Taranaki basin. In: Ministry of Commerce 1989 New Zealand Oil Exploration Conference Proceedings, pp. 1347–1353.
Schoenherr, J., Littke, R., Urai, J.L., Kukla, P.A., Rawahi, Z., 2007. Polyphase thermal evolution in the Infra-Cambrian Ara Group (South Oman Salt Basin) as deduced by maturity of solid reservoir bitumen. Org. Geochem. 38, 1293–1318. https://doi.org/10.1016/j.orggeochem.2007.03.010.
Smale, D., Mauk, J.L., Palmer, J., Soong, R., Blattner, P., 1999. Variations in sandstone diagenesis with depth, time, and space, onshore Taranaki wells, New Zealand. New Zeal. J. Geol. Geophys. 42, 137–154. https://doi.org/10.1080/00288306.1999.9514836.
Stagpoole, V., Nicol, A., 2008. Regional structure and kinematic history of a large subduction back thrust : taranaki Fault, New Zealand. J. Geophys. Res. 113, 1–19. https://doi.org/10.1029/2007JB005170.
STOS, 1984. Geological Summary Kapuni Deep-1, Taranaki, New Zealand: Unpublished New Zealand Petroleum Report 38839.
Stricker, S., Jones, S.J., Grant, N.T., 2016. Importance of vertical effective stress for reservoir quality in the Skagerrak formation, central Graben, North Sea. Mar. Petrol. Geol. 78, 895–909. https://doi.org/10.1016/j.marpetgeo.2016.03.001.
Stricker, S., Jones, S.J., Meadows, N., Bowen, L., 2018. Reservoir quality of fluvial sandstone reservoirs in salt-walled mini-basins: an example from the Seagull field, Central Graben, North Sea, UK. Petrol. Sci. 15, 1–27. https://doi.org/10.1007/s12182-017-0206-x.
Strogen, D.P., 2011. Paleogeographic Synthesis of the Taranaki Basin and Surrounds. GNS Science Report, 2010/53.
Strogen, D.P., Seebeck, H., Nicol, A., King, P.R., Cret, E., 2017. Two-phase cretaceous – paleocene rifting in the Taranaki basin region, New Zealand; implications for Gondwana break-up. J. Geol. Soc. London 174, 929–946.
Swarbrick, R.E., Osborne, M.J., Yardley, G.S., 2002. Comparison of overpressure magnitude resulting from the main generating mechanisms. In: Huffman, A.R., Bowers, G.L. (Eds.), Pressure Regimes in Sedimentary Basins and Their Prediction: AAPG Memoir 76, pp. 1–12.
Tingay, M.R.P., Hillis, R.R., Swarbrick, R.E., Morley, C.K., Damit, A.R., 2009. Origin of overpressure and pore-pressure prediction in the Baram province, Brunei. Am. Assoc. Petrol. Geol. Bull. 93, 51–74. https://doi.org/10.1306/08080808016.
Trevena, A.S., Clark, R.A., 1986. Diagenesis of Miocene gas sands in Pattani basin, Gulf of Thailand. Am. Assoc. Petrol. Geol. Bull. 70, 299–308.
Voggenreiter, W.R., 1993. Structure and evolution of the Kapuni anticline , Taranaki basin , New Zealand : evidence from the Kapuni 3D seismic survey. New Zeal. J. Geol. Geophys. 36, 77–94. https://doi.org/10.1080/00288306.1993.9514556.
Webster, M., Adams, S., 1996. Geopressures and hydrocarbon generation and migration onshore taranaki. Petrol. Explor. N. Z. News 47, 13–22.
Webster, M., O'Connor, S., Pindar, B., Swarbrick, R., 2011. Overpressures in the Taranaki basin: distribution, causes, and implications for exploration. Am. Assoc. Petrol. Geol. Bull. 95, 339–370. https://doi.org/10.1306/06301009149.
Weedman, S.D., Brantley, S.L., Albrecht, W., 1992. Secondary compaction after secondary porosity: can it form a pressure seal? Geology 20, 303–306. https://doi.org/10.1130/0091-7613(1992)020<0303:SCASPC>2.3.CO;2.
Weedman, S.D., Brantley, S.L., Shiraki, R., Poulson, S.R., 1996. Diagenesis, compaction, and fluid chemistry modeling of a sandstone near a pressure seal: lower Tuscaloosa Formation. Gulf Coast. Am. Assoc. Pet. Geol. Bull. 80, 1045–1064. https://doi.org/10.1306/64ED8C8C-1724-11D7-8645000102C1865D.
Wilkinson, M., Haszeldine, R.S., Morton, A., Fallick, A.E., Road, C., Cv, B.C., Universities, S., G, E.K., 2014. Deep burial dissolution of K-feldspars in a fluvial sandstone, pentland formation, UK central North sea. J. Geol. Soc. London 171, 635–647. https://doi.org/10.1144/jgs2013-144.
Worden, R.H., Mayall, M., Evans, I.J., 2000. The effect of Ductile-Lithic sand grains and quartz cement on porosity and permeability in Oligocene and lower Miocene clastics, South China Sea: prediction of reservoir quality. Am. Assoc. Petrol. Geol. Bull. 84, 345–359. https://doi.org/10.1306/C9EBCDE7-1735-11D7-8645000102C1865D.
Worden, R.H., Mayall, M.J., Evans, I.J., 1997. Predicting reservoir quality during exploration : lithic grains , porosity and permeability in Tertiary clastic rocks of the South China Sea basin. In: Fraser, A.J., Matthews, S.J., Murphy, R. (Eds.), Petroleum Geology of Southeast Asia. Geological Society Special Publication No. 126, pp. 107–115.